Benjamin Kollmitzer, BSc

Incoherent Optical Pumping by Means of Variational Cluster Approach

MASTER'S THESIS

For obtaining the academic degree
Diplom-Ingenieur

Master Programme of
Technical Physics

Graz University of Technology

Supervisor:
Univ.-Prof. Dr. Enrico Arrigoni
Institute of Theoretical and Computational Physics

Graz, March 7, 2012

Deutsche Fassung:
Beschluss der Curricula-Kommission für Bachelor-, Master- und Diplomstudien vom 10.11.2008
Genehmigung des Senates am 1.12.2008

EIDESSTATTLICHE ERKLÄRUNG

Ich erkläre an Eides statt, dass ich die vorliegende Arbeit selbstständig verfasst, andere als die angegebenen Quellen/Hilfsmittel nicht benutzt, und die den benutzten Quellen wörtlich und inhaltlich entnommene Stellen als solche kenntlich gemacht habe.

Graz, am …… ……..
(Unterschrift)

Englische Fassung:

STATUTORY DECLARATION

I declare that I have authored this thesis independently, that I have not used other than the declared sources / resources, and that I have explicitly marked all material which has been quoted either literally or by content from the used sources.

…… ……..
date (signature)

Abstract

Non-equilibrium Green's functions within the Keldysh formalism allow the calculation of strongly correlated quantum systems' expectation values out of equilibrium. This circumstance is vital for the correct description of Laser-driven optical microcavity-systems, since, due to dissipation, they reside in a "steady state", but not in a thermal equilibrium state.

Master equation approaches are currently prevailing in science for quantum optical systems. They allow for very accurate treatment of non-equilibrium quantum systems based on density matrices, however the computational effort grows very fast with the systems' size. Hence for spacious and correlated systems, the use of non-equilibrium Green's function methods could be advantageous.

We present three possibilities for describing incoherent optical pumping of microcavity-systems by means of cluster perturbation theory (CPT) and the more modern variational cluster approach (VCA). Every variant is analysed and its applicability examined. Furthermore, anomalies of bosonic systems are inspected using very simple models. These results are crucial for understanding each variant's difficulties.

Kurzfassung

Nichtgleichgewichts-Greensfunktionen im Keldyshformalismus erlauben die Berechnung von Erwartungswerten stark korrelierter Quantensysteme auch außerhalb des Gleichgewichts. Dieser Umstand ist entscheidend für die korrekte Beschreibung von lasergetriebenen, mikrooptischen Systemen, da sich solche aufgrund von Dissipation höchstens in einem „steady state“, nicht aber in einem thermischen Gleichgewichtszustand befinden.

Derzeit in der Wissenschaft stark verbreitet für quantenoptische Systeme sind Methoden basierend auf Mastergleichungen. Beruhend auf Dichtematrizen erlauben diese eine sehr präzise Behandlung von Nichtgleichgewichts-Quantensystemen, allerdings wächst der Aufwand stark mit der Systemgröße. Für ausgedehnte und korrelierte Systeme könnte deshalb die Verwendung von Nichtgleichgewichts-Greensfunktionen vorteilhaft sein.

Wir stellen drei Möglichkeiten vor, inkohärentes optisches Treiben von mikrooptischen Systemen mittels Cluster-Störungstheorie (cluster perturbation theory, CPT) und den moderneren variationellen Clustermethoden (variational cluster approach, VCA) zu beschreiben. Jede Variante wird einzeln analysiert und auf ihre Eignung hin untersucht. Weiters zeigen wir einige Besonderheiten bosonischer Systeme anhand von einfachen Modellen auf. Diese Ergebnisse sind entscheidend um Schwierigkeiten der gerade erwähnten Varianten verstehen zu können.

Contents

1 Introduction

Photonic crystals have been under heavy investigation since two papers from John [15] and Yablonovitch [33] in 1987. These crystals consist of periodic structures in dielectric materials. An electromagnetic wave passing through a photonic crystal experiences thus a periodically varying dielectric constant, similarly as electrons in a crystal sense a periodical coulomb potential from the lattice-atoms. Photons in a photonic crystal behave therefore analogue to electrons in a crystal, with allowed bands and band-gaps arising from the material's band-structure. A typical material for photonic crystal experiments is Gallium Arsenide (GaAs), where the crystal pattern is etched out using an electron-beam resist [11].

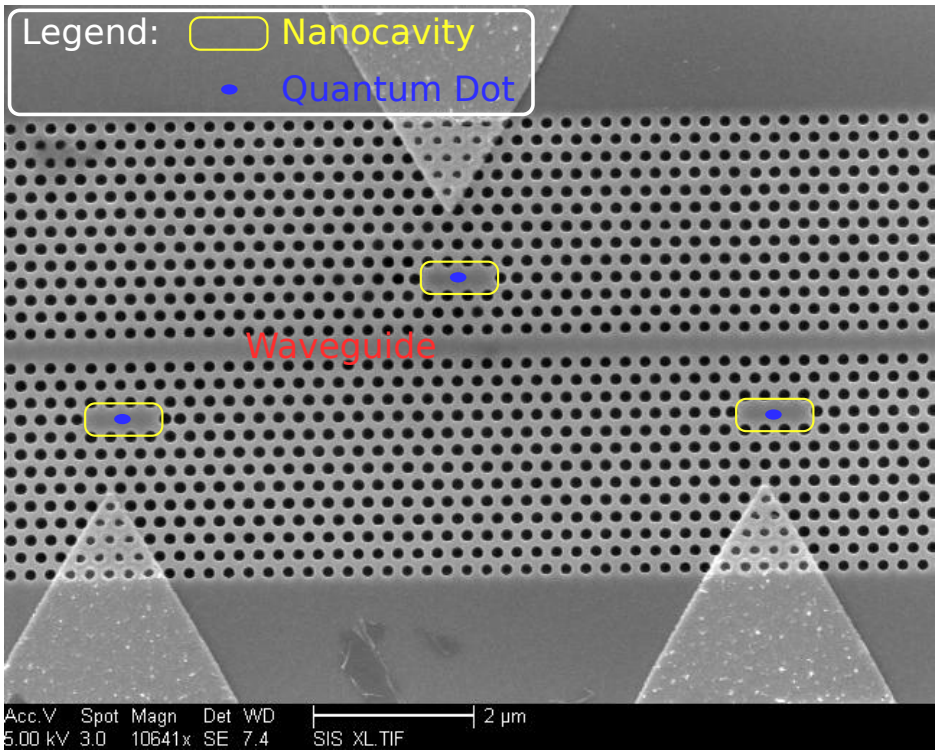

Figure 1.1: Scanning electron microscope (SEM) image of a photonic crystal. Indicated are nanocavities, supposed positions of quantum dots (not visible in SEM) and a waveguide. Andrei Faraon, Stanford University [6]

Very interesting is the possibility to confine photons to small areas of photonic crystals—so called nanocavities—by introduction of defects into the periodic structure. A few holes are left out in the photonic pattern to create such a defect site. Figure

1.2 shows the confinement of the optical field magnitude for such a nanocavity. To reduce photon losses, the first holes at the beginning and the end of the cavity are slightly shifted. In position space this corresponds to a less abrupt change in the field amplitude, while in reciprocal space the confinement is better and therefore the leakage is reduced [34]. The relatively big size of such cavities when compared to conventional crystallographic defects makes them an ideal playground for in-situ measurements and enables experimentalists to determine locally resolved observables.

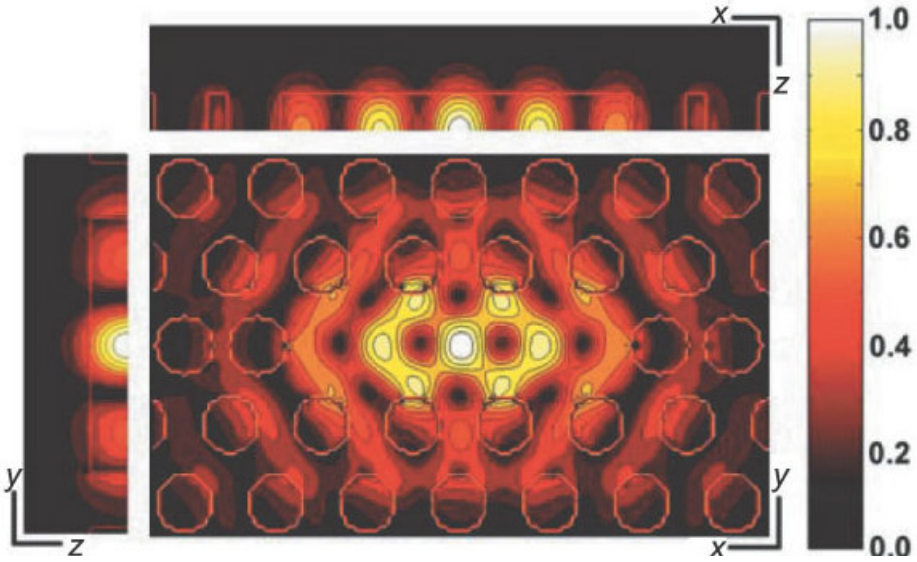

Figure 1.2: Simulated optical field magnitude $|\boldsymbol{E}|/\max|\boldsymbol{E}|$ superimposed on the nanocavity shown in Fig. 1.3 in the three primary views. The plot shows the strong confinement of the field strength to the nanocavity [34].

Due to the strong confinement of light in these cavities, strong interactions of photons with matter are possible in photonic crystals. Several groups were able to prove strong coupling between nanocavities and close by quantum dots using photoluminescence measurements [29, 34, 30, 12]. For this purpose, Laser light with a wavelength around 770 nm is focused with microscope objectives on micrometer sized spots. The light irradiance for these experiments is in the range of some $\mu\mathrm{W}/\mu\mathrm{m}^2$. The quantum dots are grown with molecular beam epitaxy in an intermediate layer of Indium Arsenide (InAs). Because of the much lower band-gap of 0.35 eV compared to GaAs with 1.42 eV, these InAs-islands act as quantum-sized potential-wells for electrons and holes. A schematic view of this set-up is given in Fig. 1.3.

More recent experiments showed further applications of photonic crystals. The group of Vučković for example was able to make a purely optical transistor using a nanocavity strongly coupled to a quantum dot and a waveguide [30] and single-photon sources based on photonic crystals [7]. Also entanglement between photons has been shown on photonic crystals only recently [3]. With these basic building blocks for quantum information processing at hand, it will be only a matter of time before small quantum networks will be realized.

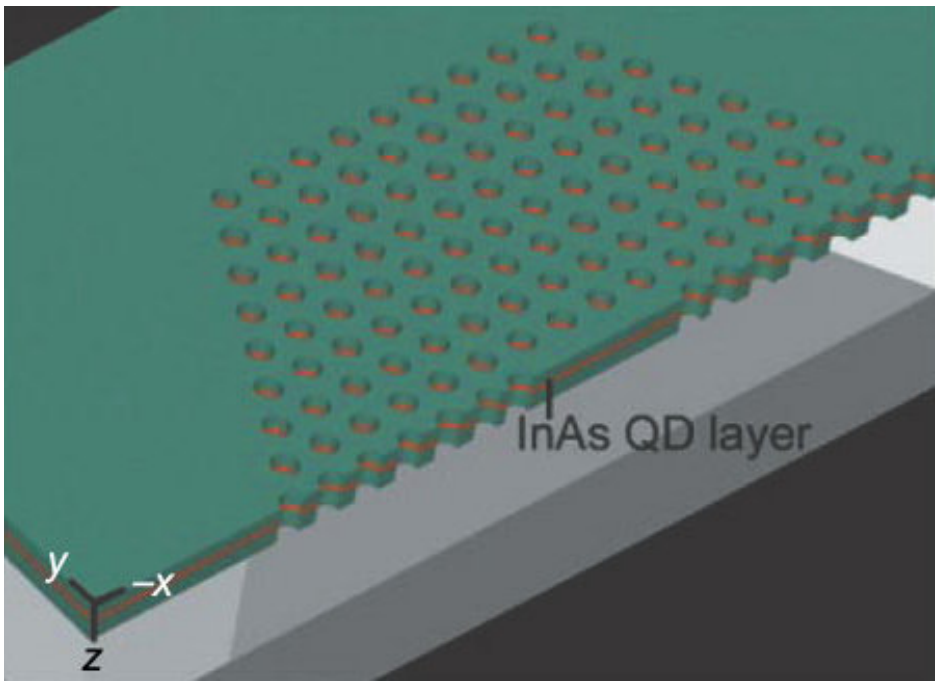

Figure 1.3: Schematic, three-dimensional view of a photonic crystal, showing strong coupling between a nanocavity and quantum dots [34]. The central area with three missing holes is the nanocavity. Quantum dots are randomly located within the red Indium Arsenide layer (InAs QD layer).

In experiments, energy is typically pumped into the probe in the form of Laser-light. Absorption- and emission-processes thus play a vital role and it is evident, that non-equilibrium methods have to be applied for correctly describing these correlated many-body phenomena. As photonic crystals can easily contain many interacting particles and possess a periodic structure, the application of methods from theoretical solid-state physics like for example cluster perturbation theory (CPT) [9, 27] and variational cluster approach (VCA) [23] would be obvious. In this thesis we try to describe optical pumping processes within the framework of these methods combined with non-equilibrium Keldysh Green's functions.

In chapter 2 we introduce the methods used within this thesis, namely Keldysh and anomalous Green's functions, as well as CPT. Apart from 2.3, which consists of new information worked out during this thesis in our group [18], this section is a summary of textbook-knowledge and scientific papers. Chapter 4 contains our own treatment and results concerning optical pumping. Of course, some difficulties, which we did not understand right away, emerged in these calculations. They are examined in chapter 3, where we treat small and easy to solve systems showing similar characteristics. These simple calculations are comparable to exercises in quantum-mechanics courses and can therefore be found in text-books, however some procedures of solution might be novel.

2 Methods

Numerous techniques are available to study the behaviour of quantum mechanical correlated many-body systems, for example Dynamical Mean-Field Theory (DMFT) or Quantum Monte Carlo. In this work we discuss CPT and VCA for non-equilibrium systems. We follow [20] and [5] for equilibrium Green's functions' definitions, properties and observables, [24] and [16] for non-equilibrium Green's functions, [10] for currents and [27, 28, 26] for CPT.

2.1 Non-equilibrium Green's Functions

2.1.1 Definitions

The connection between experimentally measurable quantities and theory can be made elegantly by using Green's functions [20, pp. 49–53], also referred to as correlation functions or propagators. The most common two-body Green's functions are the time-ordered G, retarded G^R and advanced G^A. These are defined for bosons (commutator) and fermions (anticommutator) as [5, p. 254]

$$G(i,t_i;\,j,t_j) = -\mathrm{i}\langle T\left[c_i(t_i)\,c_j^\dagger(t_j)\right]\rangle \tag{2.1}$$

$$G^R(i,t_i;\,j,t_j) = -\mathrm{i}\theta(t_i-t_j)\langle\left[c_i(t_i),c_j^\dagger(t_j)\right]_\mp\rangle \tag{2.2}$$

$$G^A(i,t_i;\,j,t_j) = \mathrm{i}\theta(t_j-t_i)\langle\left[c_i(t_i),c_j^\dagger(t_j)\right]_\mp\rangle \tag{2.3}$$

respectively, where T denotes the time-ordering operator, $\theta(t)$ the Heaviside step function, $\langle O\rangle$ the expectation value of O, $[A,B]_\mp$ the commutator $(-)$ and anticommutator $(+)$, $c_i(t_i)$ the annihilation- and $c_i^\dagger(t_i)$ the creation-operator at position i and time t_i. The time-ordering ensures, that the operator with the smaller time argument stands on the right hand side, id est acts first. If two fermionic operators are swapped by T, an additional minus sign has to be taken into account. The creation- and annihilation-operators at $t=0$ obey by definition the following commutator relationships

$$\left[c_i,c_j^\dagger\right]_\mp \equiv c_ic_j^\dagger \mp c_j^\dagger c_i = \delta_{i,j}, \tag{2.4}$$

$$[c_i,c_j]_\mp = 0, \qquad \left[c_i^\dagger,c_j^\dagger\right]_\mp = 0, \tag{2.5}$$

where the Kronecker delta $\delta_{i,j}=1$ for $i=j$ and zero else was introduced.

To distinguish between equilibrium and non-equilibrium expressions, we use capital G for the general case and small letter g for equilibrium Green's functions. This means expressions with small letter Green's functions are only valid in equilibrium.

While it is usually sufficient to work with retarded Green's functions in equilibrium problems, where all times are equivalent and the occupation probabilities are given by the Bose or Fermi-Dirac distributions, it is necessary to introduce another Green's function in the non-equilibrium case. One generally chooses the Keldysh Green's function [24, 16]

$$G^K(i,t_i;\,j,t_j) = -\mathrm{i}\langle\left[c_i(t_i), c_j^\dagger(t_j)\right]_\pm\rangle. \tag{2.6}$$

The retarded, advanced and Keldysh Green's functions can be combined into a matrix notation called Keldysh space to give a Green's function matrix

$$\hat{G} = \begin{pmatrix} G^R & G^K \\ 0 & G^A \end{pmatrix}, \tag{2.7}$$

whose usefulness will be manifest in chapter 2.2. One should note, that multiplication and inversion can be easily performed and preserve the Keldysh structure.

$$\hat{G}\hat{F} = \begin{pmatrix} G^R F^R & G^R F^K + G^K F^A \\ 0 & G^A F^A \end{pmatrix} \tag{2.8}$$

$$\hat{G}^{-1} = \begin{pmatrix} \left(G^R\right)^{-1} & -\left(G^R\right)^{-1} G^K \left(G^A\right)^{-1} \\ 0 & \left(G^A\right)^{-1} \end{pmatrix} \tag{2.9}$$

In steady state, the Green's functions depend only on the time difference $\tau = t_i - t_j$ because of time translation invariance as in equilibrium. However the occupation probabilities are not given by the Bose or Fermi-Dirac distributions in general. For calculations it is often convenient to Fourier transform the Green's functions with respect to τ, according to [20, p. 148]

$$G(\omega) = \int_{-\infty}^{\infty} \mathrm{d}\tau\, e^{\mathrm{i}\omega\tau} G(\tau). \tag{2.10}$$

A very handy identity for performing the transformation is given on the same page, namely

$$\int_{-\infty}^{\infty} \mathrm{d}\tau\, \exp\left(\mathrm{i}\tau(\omega \pm \mathrm{i}\Gamma)\right)\theta(\pm\tau) = \frac{\pm\mathrm{i}}{\omega \pm \mathrm{i}\Gamma}, \qquad \text{for } \Gamma > 0 \tag{2.11}$$

where the $\pm\mathrm{i}\Gamma$ (depending on the sign in the theta-distribution's argument) is necessary for convergence. For example $\theta(-\tau) = 1$ for $\tau < 0$, but the exponent $-\mathrm{i}^2\tau\Gamma = \tau\Gamma$ ensures that the integrand vanishes for $\tau \to -\infty$. For free particles, one generally has $\Gamma = 0^+$, which means the "limit $\Gamma \to 0^+$ after evaluation"

$$\int_{-\infty}^{\infty} \mathrm{d}\tau\, \exp\left(\mathrm{i}\tau\omega\right)\theta(\pm\tau) = \frac{\pm\mathrm{i}}{\omega \pm \mathrm{i}0^+}. \tag{2.12}$$

2.1.2 Q-Matrix Representation

The perturbative calculations described in chapter 2.2 and used within this thesis are performed in frequency-space because of time-translational invariance in equilibrium- and steady-state. However, for evaluating observables like particle-densities and currents beginning from frequency-space expressions, an inverse transformation to the time-domain has to be performed. We use the Q-matrix representation because it is very convenient for integrating Green's functions, which corresponds to this inverse transformation.

We treat only the case, where a system described by its Hamiltonian $\mathcal{H}$ is initially prepared in its N-particle eigenstate $|\psi_\sigma^N\rangle$. The sub-index σ labels the eigenstates according to their grand-canonical eigenvalue $\langle\psi_\sigma^N|\mathcal{H}-\mu N|\psi_\sigma^N\rangle$, where μ is the chemical potential and N the particle number operator. During this calculation we treat σ as arbitrary, but fixed. It is used in later chapters to calculate Green's functions for systems, which are initially prepared in an excited state.

For $\sigma = 0$, which is the ground-state, we end up in the usual $T = 0$ equilibrium situation. However, generalizations to finite temperature equilibrium-states are straight forward by substituting expectation values

$$\langle\psi_0^N|\hat{O}|\psi_0^N\rangle \qquad \rightarrow \qquad \mathrm{tr}\,\hat{\rho}\hat{O}, \tag{2.13}$$

where we introduced the density-matrix operator

$$\hat{\rho} = \frac{1}{Z}\exp\left(-\beta(\mathcal{H}-\mu N)\right), \tag{2.14}$$

the grand canonical partition function $Z = \mathrm{tr}\exp\left(-\beta(\mathcal{H}-\mu N)\right)$ and the inverse temperature $\beta = 1/k_B T$.

By inserting a complete set of eigenstates $\sum_\gamma |\psi_\gamma\rangle\langle\psi_\gamma|$ of the Hamiltonian into Eqs. (2.1)–(2.3) and performing a subsequent Fourier transformation, one can derive the so-called Lehmann representation [20, pp. 240–242]

$$G(i,j;\omega) = \sum_\alpha \frac{\langle\psi_\sigma^N|c_i|\psi_\alpha^{N+1}\rangle\langle\psi_\alpha^{N+1}|c_j^\dagger|\psi_\sigma^N\rangle}{\omega - \Delta E_\alpha + \zeta\cdot \mathrm{i}0^+} \mp \sum_\beta \frac{\langle\psi_\sigma^N|c_j^\dagger|\psi_\beta^{N-1}\rangle\langle\psi_\beta^{N-1}|c_i|\psi_\sigma^N\rangle}{\omega + \Delta E_\beta + \xi\cdot \mathrm{i}0^+}, \tag{2.15}$$

where the energy E_σ of the N-particle initial state $|\psi_\sigma^N\rangle$, the energy difference $\Delta E_\gamma = E_\gamma - E_\sigma$ and

$$\zeta = \begin{cases} +1 \\ +1\,, \\ -1 \end{cases} \qquad \xi = \begin{cases} -1 & \text{time-ordered} \\ +1\,, & \text{for} \quad \text{retarded} \\ -1 & \text{advanced} \end{cases} \tag{2.16}$$

where introduced. The sums extend over the $(N \pm 1)$-particle eigenstates $|\psi_{\alpha/\beta}^{N\pm1}\rangle$.

The same procedure of inserting eigenstates into Eq. (2.6) and Fourier transforming leads to the Lehmann representation of the Keldysh Green's function

$$\frac{\mathrm{i}G^K(i,j;\omega)}{2\mathrm{i}0^+} = \sum_\alpha \frac{\langle\psi_\sigma^N|c_i|\psi_\alpha^{N+1}\rangle\langle\psi_\alpha^{N+1}|c_j^\dagger|\psi_\sigma^N\rangle}{(\omega-\Delta E_\alpha)^2 - (0^+)^2} \pm \sum_\beta \frac{\langle\psi_\sigma^N|c_j^\dagger|\psi_\beta^{N-1}\rangle\langle\psi_\beta^{N-1}|c_i|\psi_\sigma^N\rangle}{(\omega+\Delta E_\beta)^2 - (0^+)^2}. \tag{2.17}$$

To calculate expectation values like particle densities or currents, one has to carry out integrations with respect to ω. During such calculations, the numerators and the energy differences stay the same and only ω changes. It is therefore practical to rewrite Eqs. (2.15) and (2.17) as matrix-multiplication [17]

$$G^R(\omega) = Q(\omega + \mathrm{i}0^+ - \boldsymbol{\lambda})^{-1} S Q^\dagger \tag{2.18}$$

$$G^K(\omega) = -2\mathrm{i}0^+ Q \left((\omega - \boldsymbol{\lambda})^2 + (0^+)^2\right)^{-1} T Q^\dagger \tag{2.19}$$

with

$$Q^\dagger_{\alpha,j} = \langle \psi^{N+1}_\alpha | c^\dagger_j | \psi^N_\sigma \rangle \qquad Q^\dagger_{\beta,j} = \langle \psi^N_\sigma | c^\dagger_j | \psi^{N-1}_\beta \rangle \tag{2.20}$$

$$\lambda_\alpha = \Delta E_\alpha \qquad \lambda_\beta = -\Delta E_\beta \tag{2.21}$$

$$S = \mathrm{diag}(+1 \quad +1 \quad \ldots \quad \mp 1 \quad \mp 1 \quad \ldots) \tag{2.22}$$

$$T = \mathrm{diag}(\underbrace{+1 \quad +1 \quad \ldots}_{\text{for } \alpha} \quad \underbrace{\pm 1 \quad \pm 1 \quad \ldots}_{\text{for } \beta}) \tag{2.23}$$

for the bosonic $(-)$ and fermionic $(+)$ case.

A very useful result for checking Q-matrix calculations can be derived as follows,

$$\begin{aligned} \left(Q \cdot S \cdot Q^\dagger\right)_{i,j} &= \sum_\gamma Q_{i,\gamma} S_{\gamma,\gamma} Q^\dagger_{\gamma,j} \\ &= \sum_\alpha \langle \psi^N_0 | c_i | \psi^{N+1}_\alpha \rangle \langle \psi^{N+1}_\alpha | c^\dagger_j | \psi^N_0 \rangle \mp \sum_\beta \langle \psi^{N-1}_\beta | c_i | \psi^N_0 \rangle \langle \psi^N_0 | c^\dagger_j | \psi^{N-1}_\beta \rangle \\ &= \langle \psi^N_0 | c_i c^\dagger_j \mp c^\dagger_j c_i | \psi^N_0 \rangle \overset{(2.4)}{=} \delta_{i,j}. \end{aligned} \tag{2.24}$$

2.1.3 Keldysh Green's Function in Equilibrium

It is possible to derive a relationship between retarded, advanced and Keldysh Green's functions in equilibrium. Equations (2.1)–(2.6) can be rewritten to give

$$G^K = 2G - G^R - G^A. \tag{2.25}$$

By taking into account [20, pp. 241–247]

$$\mathrm{Re}\, g^R(\omega) = \mathrm{Re}\, g^A(\omega) = \mathrm{Re}\, g(\omega) \tag{2.26}$$

$$\mathrm{Im}\, g^R(\omega) = -\,\mathrm{Im}\, g^A(\omega) = \mathrm{Im}\, g(\omega) \cdot \tanh^{\pm 1}\left(\beta \frac{\omega - \mu}{2}\right), \tag{2.27}$$

the time ordered and advanced Green's functions in Eq. (2.25) can be substituted, resulting in

$$g^K = 2\,\mathrm{Im}\, g^R \cdot \tanh^{\mp 1}\left(\beta \frac{\omega - \mu}{2}\right). \tag{2.28}$$

For zero temperature, this expression reduces to

$$g^K = 2 \operatorname{Im} g^R \cdot \operatorname{sgn}(\omega - \mu). \tag{2.29}$$

Because these relations are so often used, we abbreviate

$$\tanh^{\mp 1}\left(\beta \frac{\omega - \mu}{2}\right) \equiv s(\omega). \tag{2.30}$$

2.1.4 Properties

To obtain the analytical properties of the Green's functions, one can analyse Eqs. (2.15) or (2.18). The retarded Green's function has poles just below the real axis $z = \lambda_\gamma - \mathrm{i}0^+$ and is analytic continuable in the upper half plane $\operatorname{Im} z \geq 0$. Equivalently, the advanced Green's function has poles just above the real axis and is analytic in the lower half plane $\operatorname{Im} z \leq 0$ [20, p. 242].

Alternatively, one might say the poles of the Green's functions reside on the real axis. The retarded (advanced) Green's function would then be defined on a line just above (below) these poles and analytical continuable in $z \in \mathbb{C} \backslash \{\lambda_\gamma\}$.

This property can be used to transform integration contours. For example, it is possible to integrate the retarded Green's function over the positive imaginary axis instead of the real axis for evaluating particle densities. This is handy, as the features on the real axis are far more peaked and harder to approximate numerically.

The analytical properties can also be used to check the correctness of calculations. A useful relation for this purpose is for example

$$\int_{-\infty}^{\infty} \mathrm{d}\omega \, p(\omega) \cdot G^R(\omega) = 0, \tag{2.31}$$

for an in the upper half plane $\operatorname{Im} z \geq 0$ analytical function $p(z)$, which vanishes at least like $\frac{1}{z}$ for $z \to \infty$. Of course, this relation is a necessary but not sufficient condition for correctness because it can also be fulfilled by chance for non-causal Green's functions.

Proof. Because G^R is analytical for $\operatorname{Im} z \geq 0$,

$$\oint_C \mathrm{d}z \, p(z) \cdot G^R(z) = 0 \tag{2.32}$$

for every analytical function $p(z)$ and closed integration contour C on the upper half plane. If $p(z)$ vanishes at least like $G^R(z) \propto \frac{1}{z}$ for $z \to \infty$ (compare Eq. (2.15)), we can choose our contour along the real axis and close it via a semicircle at infinity, as shown in Fig. 2.1. Because of the $(\frac{1}{z})^2$ behaviour of $p(z) \cdot G^R(z)$ for large z, the part along the semicircle vanishes and we are left with Eq. (2.31). □

Another handy relation for checking calculations is the so called sum rule [5, p. 265]

$$\int_{-\infty}^{\infty} \frac{\mathrm{d}\omega}{2\pi} \, \mathrm{i} \left(G^R(\omega) - G^A(\omega) \right) = \mathbb{I}, \tag{2.33}$$

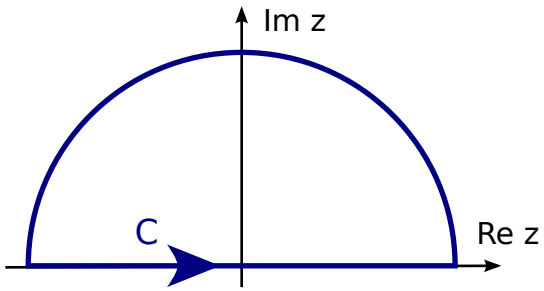

Figure 2.1: Integration contour C.

which follows from the commutator relationships of creation- and annihilation-operators Eq. (2.4), the Green's function definitions Eqs. (2.2) and (2.3) for time translation invariance and the inverse Fourier transform, as

$$\begin{aligned} \mathbb{I} \equiv \delta_{i,j} \overset{(2.4)}{=} \left[c_i, c_j^\dagger\right]_\mp &= \mathrm{i}\left(G^R(\tau=0) - G^A(\tau=0)\right) \\ &= \int_{-\infty}^{\infty} \frac{\mathrm{d}\omega}{2\pi}\, \mathrm{i}\left(G^R(\omega) - G^A(\omega)\right) \\ &= \int_{-\infty}^{\infty} \frac{\mathrm{d}\omega}{2\pi}\, A(\omega). \end{aligned} \tag{2.34}$$

In the last line we have introduced a DOS-like (density of states) quantity [5, p. 264]

$$A(\omega) = \mathrm{i}\left(G^R(\omega) - G^A(\omega)\right). \tag{2.35}$$

The Keldysh Green's function is neither analytical in the upper, nor in the lower half plane. This can be seen from Eq. (2.25), where the Keldysh Green's function is written as a linear combination of G^R and G^A. As stated before, G^R is analytical in the upper half plane, where G^A has poles and vice versa. Therefore G^K has poles in both half planes, as shown in Fig. 2.2. These poles make most integration path deformations impractical.

2.1.5 Observables

We are especially interested in calculating particle densities and currents. While densities are available in equilibrium as well, currents are typically a non-equilibrium phenomena. We will therefore derive an equilibrium and a non-equilibrium relation for the particle densities in this section. We follow [10] for the current and [24, 5] for particle densities.

By using the definition of G^K Eq. (2.6) and the commutator relationship Eq. (2.4),

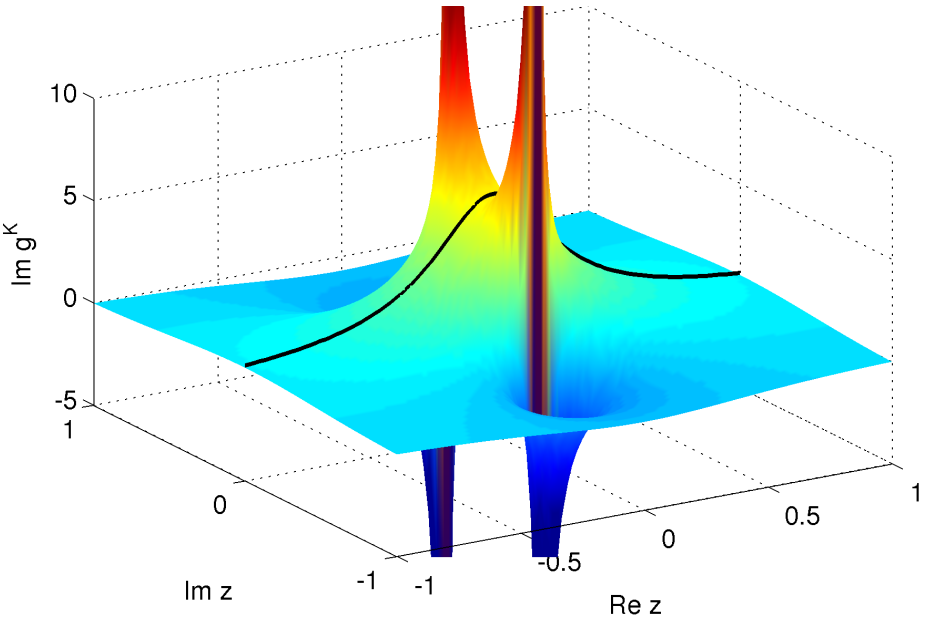

Figure 2.2: Imaginary part of the equilibrium Keldysh Green's function $g^K(\lambda + z)$ in the vicinity of an excitation λ, plotted in the complex plane $z \in \mathbb{C}$ for $0^+ = 0.3$. The black solid line indicates an integration contour along the real axis.

we can rewrite

$$\begin{aligned} \pm\left(\frac{\mathrm{i}}{2}G^K(i,i;\,t=0)-\frac{1}{2}\right) &\overset{(2.6)}{=} \pm\frac{1}{2}\left(\langle c_i c_i^\dagger\rangle \pm \langle c_i^\dagger c_i\rangle - 1\right) \\ &\overset{(2.4)}{=} \pm\frac{1}{2}\left(1 \pm \langle c_i^\dagger c_i\rangle \pm \langle c_i^\dagger c_i\rangle - 1\right) \\ &= \langle c_i^\dagger c_i\rangle = n_i, \end{aligned} \tag{2.36}$$

to yield the particle density in the general case. The $t = 0$ Keldysh Green's function can be calculated by integrating $G^K(\omega)$ over the real axis

$$G^K(i,j;\,t=0) = \int_{-\infty}^{\infty}\frac{\mathrm{d}\omega}{2\pi}\,G^K(i,j;\,\omega), \tag{2.37}$$

like indicated in Fig. 2.2.

The equilibrium particle density, as shown in [5, pp. 264,270], can be expressed as

$$n_i = \langle c_i^\dagger c_i\rangle = \int_{-\infty}^{\infty}\frac{\mathrm{d}\omega}{2\pi}\,A(i,i;\,\omega)\cdot f_\mp(\omega), \tag{2.38}$$

with the Bose-Einstein (Fermi-Dirac) distribution

$$f_\mp(\omega) = \frac{1}{\exp\left(\beta(\epsilon_r-\mu)\right)\mp 1}, \tag{2.39}$$

which is a function of frequency ω, as well as the inverse temperature $\beta = 1/k_B T$ and the chemical potential μ.

Haug and Jauho derive in their book [10, pp. 186–187] a formula for the current density $I_{i,j}$ between neighbouring sites i and j with the electrical charge q, namely

$$I_{i,j} = -\mathrm{i}qV \left(\langle c_i^\dagger c_j \rangle - \langle c_j^\dagger c_i \rangle \right). \tag{2.40}$$

With the help of Eqs. (2.2), (2.3) and (2.6) and the fact $\mathrm{i}\langle c_i^\dagger c_j \rangle = -(\mathrm{i}\langle c_j^\dagger c_i \rangle)^*$, we can transform this relation into

$$I_{i,j} = \pm qV \,\mathrm{Re}\, G^K(i,j;\, t=0). \tag{2.41}$$

2.2 Perturbative Methods

Usually one is interested in systems, which are too hard to solve exactly (otherwise they are most likely already solved). One way to tackle such problems is to split them into separate, manageable parts and combine these perturbatively. In this chapter we present a well established perturbative approach using Green's functions.

For a specific class of Hamiltonians $\mathcal{H} = \mathcal{H}_0 + V$, consisting of one interacting, but at least numerically solvable system $\mathcal{H}_0 = \sum_m \mathcal{H}_{0,m}$ and a quadratic coupling term

$$V = \sum_{m,n} \sum_{\substack{i \in m \\ j \in n}} V_{i,j} c_i^\dagger c_j, \tag{2.42}$$

strong-coupling perturbation theory yields a useful result for the total system's Green's function up to lowest-order contributions

$$G^{-1} \equiv G_0^{-1} - \Sigma \approx G_0^{-1} - V. \tag{2.43}$$

Notice that higher order contributions are not as easy to evaluate due to the lack of Wick's theorem. In Eq. (2.43), m, n label individual clusters which are independent from each other within $\mathcal{H}_0$, while i and j sum over a convenient basis. The first equation defines the self-energy Σ and is called Dyson's equation in the literature [20, pp. 111–113], [5, pp. 300–306], while the overall approximative scheme was originally introduced by Gros and Valenti in 1993 [9] and was named cluster perturbation theory (CPT) by Sénéchal et al. in the year 2000 [27]. An in-depth derivation can be found in [28], while more introductory lecture notes are available on the arXiv [26].

The theory behind CPT builds on the following chronological sequence: At $t \to -\infty$, the total system is taken to be in the ground-state $|\Psi_0\rangle$ determined by $\mathcal{H}_0$. The perturbation V is then switched on adiabatically, meaning slow enough that the system can always relax into its current ground-state. When V is fully applied, it is therefore located in the ground-state given approximately by $\mathcal{H}$ and measurements of all the interesting quantities are feasible. Afterwards, V gets again adiabatically switched off, so that at $t \to \infty$ the system resides—apart from phase factors—again in $|\Psi_0\rangle$.

The total Hamiltonian $\mathcal{H}$ describes in usual applications an infinite lattice with interacting regions, meaning more than quadratic in creation- and annihilation-operators. Because of this interaction, $\mathcal{H}$ cannot be easily diagonalized, but is split into smaller clusters $\mathcal{H}_{0,m}$. The bonds between these clusters are accounted for by V. An illustration of this procedure is given in Fig. 2.3.

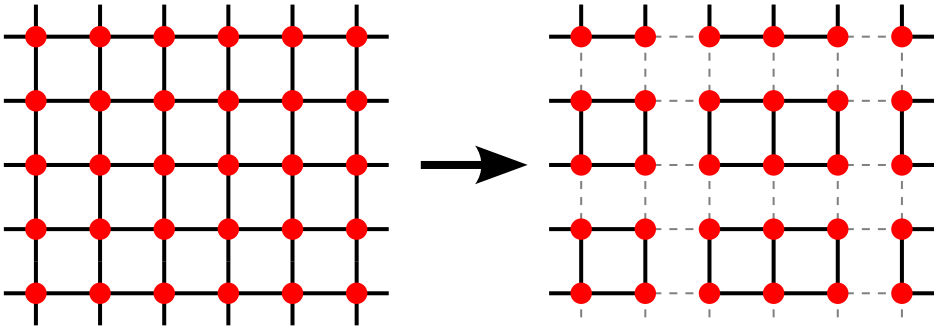

Figure 2.3: Splitting of total Hamiltonian $\mathcal{H}$ (left) into individual clusters $\mathcal{H}_{0,m}$ (right). The dashed lines represent the inter-cluster bonds V.

The procedure of adiabatically switching the perturbation on and off again— although being necessary for CPT in equilibrium—is inconvenient in non-equilibrium, as we want to be able to treat problems like for example quantum-quenches, where the perturbation is switched on instantaneously. Using the Keldysh space Green's function matrices Eq. (2.7), one can derive the very same result as Eq. (2.43) for steady state in frequency domain [10, 24, 19]

$$\hat{G}^{-1}(\omega) = \hat{G}_0^{-1}(\omega) - \hat{V}, \tag{2.44}$$

where we have taken into account, that V does not depend on the frequency and introduced $\hat{V} = \mathrm{diag}\begin{pmatrix} V & V \end{pmatrix}$. The inversion of the Keldysh space matrices simplify Eq. (2.44) to

$$\left(G^{R/A}\right)^{-1} = \left(G_0^{R/A}\right)^{-1} - V, \tag{2.45}$$

$$G^K = -G^R \left(\hat{G}_0^{-1}\right)^K G^A, \tag{2.46}$$

where $(\hat{G}_0^{-1})^K$ denotes the Keldysh component of $\hat{G}_0^{-1}$.

Example We treat two clusters $m \in \{\alpha, \beta\}$ and rearrange the notation for the Green's functions

$$\hat{G} = \begin{pmatrix} \hat{G}_{\alpha,\alpha} & \hat{G}_{\alpha,\beta} \\ \hat{G}_{\beta,\alpha} & \hat{G}_{\beta,\beta} \end{pmatrix}, \qquad \hat{G}_0 = \begin{pmatrix} \hat{G}_{0\,\alpha,\alpha} & \\ & \hat{G}_{0\,\beta,\beta} \end{pmatrix}, \qquad \hat{V} = \begin{pmatrix} & \hat{V}_{\alpha,\beta} \\ \hat{V}_{\beta,\alpha} & \end{pmatrix}, \tag{2.47}$$

where each element is a Keldysh space and cluster site matrix. We have also set all intra-cluster elements of the perturbation zero

$$V_{i,j} \equiv 0 \quad \forall i, j \in m, \tag{2.48}$$

to ease the calculational effort. Note that it is always possible to incorporate inter-cluster elements of V (which are by definition only quadratic in c and $c^\dagger$) into the unperturbed $\mathcal{H}_{0,m}$, which is in fact the principle used for a more general method called variational-CPT or variational cluster approach (VCA) [23].

This enables us to readily evaluate Eq. (2.44)

$$\hat{G}^{-1}_{\alpha,\alpha} = \hat{G}^{-1}_{0\,\alpha,\alpha} - \hat{V}_{\alpha,\beta} \cdot \hat{G}_{0\,\beta,\beta} \cdot \hat{V}_{\beta,\alpha}, \tag{2.49}$$

$$\hat{G}_{\alpha,\beta} = \hat{G}_{\alpha,\alpha} \cdot \hat{V}_{\alpha,\beta} \cdot \hat{G}_{0\,\beta,\beta}. \tag{2.50}$$

From Eqs. (2.8) and (2.9) we know, that the retarded and advanced parts do not mix in these operations. They obey therefore the same relations as the Keldysh matrices

$$\left(G^{R/A}_{\alpha,\alpha}\right)^{-1} = \left(G^{R/A}_{0\,\alpha,\alpha}\right)^{-1} - V_{\alpha,\beta} \cdot G^{R/A}_{0\,\beta,\beta} \cdot V_{\beta,\alpha}, \tag{2.51}$$

$$G^{R/A}_{\alpha,\beta} = G^{R/A}_{\alpha,\alpha} \cdot V_{\alpha,\beta} \cdot G^{R/A}_{0\,\beta,\beta}. \tag{2.52}$$

Only the Keldysh components differ, but as the perturbations $\hat{V}$ contain no Keldysh components, they are also easily evaluated

$$G^{K}_{\alpha,\alpha} = G^{R}_{\alpha,\alpha} \left(\left(\hat{G}^{-1}_{0\,\alpha,\alpha}\right)^{K} - V_{\alpha,\beta} \cdot G^{K}_{0\,\beta,\beta} \cdot V_{\beta,\alpha} \right) G^{A}_{\alpha,\alpha}, \tag{2.53}$$

$$G^{K}_{\alpha,\beta} \overset{(2.8)}{=} G^{R}_{\alpha,\alpha} \cdot V_{\alpha,\beta} \cdot G^{K}_{0\,\beta,\beta} + G^{K}_{\alpha,\alpha} \cdot V_{\alpha,\beta} \cdot G^{A}_{0\,\beta,\beta}. \tag{2.54}$$

We can rewrite the Keldysh component of the inverse unperturbed Green's function $(G_{0\,\alpha,\alpha})^{-1}$ for equilibrium conditions before applying the perturbation using Eq. (2.28) as

$$\begin{aligned} \left(\hat{g}^{-1}_{0\,\alpha,\alpha}\right)^{K} &\overset{(2.9)}{=} -\left(g^{R}_{0\,\alpha,\alpha}\right)^{-1} g^{K}_{0\,\alpha,\alpha} \left(g^{A}_{0\,\alpha,\alpha}\right)^{-1} \\ &\overset{(2.28)}{=} \left(\left(g^{R}_{0\,\alpha,\alpha}\right)^{-1} - \left(g^{A}_{0\,\alpha,\alpha}\right)^{-1} \right) \cdot s_\alpha(\omega). \end{aligned} \tag{2.55}$$

This relation simplifies the calculation of the Keldysh Green's function tremendously. It can be used whenever one limits oneself to tile $\mathcal{H}$ into an equilibrium part $\mathcal{H}_0$ and considers all non-equilibrium properties to be part of the perturbation V. ∎

2.3 Anomalous Green's Functions

In this chapter we follow [18] for the Q-matrix formalism of the retarded Green's function. However, the Q-matrix formalism for the non-equilibrium Keldysh Green's function is novel.

When the system's Hamiltonian $\mathcal{H}$ does not commute with the particle number operator N, they share no common set of eigenvectors. That means, the eigenvectors are in general linear combinations of basis states with *different* particle numbers. Products like $\langle\psi_\sigma|c|\psi_\sigma\rangle$ can therefore be finite.

Such Hamiltonians are typical for superfluid systems and are said to have a broken U(1) symmetry. This fact can be easily understood if one takes into account, that U(1) corresponds to $e^{\mathrm{i}\varphi}$ with $\varphi \in \mathbb{R}$.

Example Let us investigate, how two Hamiltonians, $\mathcal{H}'$ which commutes with N and $\mathcal{H}$ which does not, behave under a U(1) transformation $c \to c \cdot e^{\mathrm{i}\varphi}$.

$$\begin{aligned} \mathcal{H}' &\propto c^\dagger c = N & \mathcal{H} &\propto c^\dagger + c \\ &\to c^\dagger e^{-\mathrm{i}\varphi} \cdot c e^{\mathrm{i}\varphi} = c^\dagger c & &\to c^\dagger e^{-\mathrm{i}\varphi} + c e^{\mathrm{i}\varphi} \end{aligned}$$

While $\mathcal{H}$ does change under this transformation, $\mathcal{H}'$ does not, id est it has U(1) symmetry. ∎

One consequence of this not commuting with N is that in the Lehmann representation Eq. (2.15), the sums have to be expanded from containing only $(N \pm 1)$-particle eigenstates to extend over all $n_s + 1$ eigenstates $|\psi_\gamma\rangle$ of the Hamiltonian

$$G(i,j;\omega) = \sum_{\gamma=0}^{n_s} \frac{\langle\psi_\sigma|c_i|\psi_\gamma\rangle\langle\psi_\gamma|c_j^\dagger|\psi_\sigma\rangle}{\omega - \Delta E_\gamma + \zeta \cdot \mathrm{i}0^+} \mp \sum_{\gamma=0}^{n_s} \frac{\langle\psi_\sigma|c_j^\dagger|\psi_\gamma\rangle\langle\psi_\gamma|c_i|\psi_\sigma\rangle}{\omega + \Delta E_\gamma + \xi \cdot \mathrm{i}0^+}. \tag{2.56}$$

If the initial state $|\psi_\sigma\rangle$ contains only basis states with equal particle numbers, so-called anomalous expectation values $\langle cc\rangle$ and $\langle c^\dagger c^\dagger\rangle$ are always zero. This is however not the case for broken U(1) symmetry. It is therefore also necessary to take these expectation values in form of anomalous Green's functions $\mathcal{F}$ into account. Formally one introduces a Nambu notation $\mathcal{G}$, containing regular particle G, hole $\bar{G}$ and anomalous $\mathcal{F}^{(\dagger)}$ Green's functions

$$\mathcal{G}(i,t_i;\, j,t_j) = \begin{pmatrix} G & \mathcal{F} \\ \mathcal{F}^\dagger & \bar{G} \end{pmatrix} = \begin{pmatrix} G(c_i(t_i), c_j^\dagger(t_j)) & G(c_i(t_i), c_j(t_j)) \\ G(c_i^\dagger(t_i), c_j^\dagger(t_j)) & G(c_i^\dagger(t_i), c_j(t_j)) \end{pmatrix}, \tag{2.57}$$

where every element has to be again a 2-by-2 Keldysh matrix for treating non-equilibrium problems. By substituting (i,t_i) for (j,t_j) and vice versa in the Green's functions definitions Eqs. (2.2)–(2.3), it is easily shown that $\bar{G}_{i,j}^{R/A}$ can be written as $\pm G_{j,i}^{A/R}$ for bosons (+) and fermions (−). That means in frequency notation

$$\bar{G}^{R/A}(i,j;\omega) = \pm G^{A/R}(j,i;-\omega) \tag{2.58}$$

because the exchange of the time arguments transforms $\omega + \mathrm{i}0^+$ to $-(\omega + \mathrm{i}0^+) = -\omega - \mathrm{i}0^+$.

Harder is the calculation of the hole Keldysh Green's function. As the number operator N and the Hamiltonian $\mathcal{H}$ do not commute, they share no common set of eigenstates. It is therefore not trivial to fill the system up to a certain energy using a finite chemical potential, as is the common procedure for particle-number conserving quantum-systems. We will hence set the chemical potential to zero if $\mathcal{H}$ and N do not commute. With this simplification, the hole Keldysh Green's function can be calculated like the retarded to be

$$\bar{G}^K(i,j;\omega) = \pm G^K(j,i;-\omega), \tag{2.59}$$

and in equilibrium

$$\bar{g}^K(\omega) = 2\,\mathrm{Im}\,\bar{g}^R(\omega)\cdot\mathrm{sgn}(-\omega). \tag{2.60}$$

The Q-matrix formalism can be applied similarly as in chapter 2.1.2 for calculating the full Nambu matrix Green's function [18]

$$\mathcal{G}^R(\omega) = Q(\omega + \mathrm{i}0^+ - \boldsymbol{\lambda})^{-1} S Q^\dagger \tag{2.61}$$

$$\mathcal{G}^K(\omega) = -2\mathrm{i}0^+ Q\left((\omega - \boldsymbol{\lambda})^2 + (0^+)^2\right)^{-1} T Q^\dagger \tag{2.62}$$

with

$$Q = \begin{pmatrix} R & Z \\ Z^* & R^* \end{pmatrix} \tag{2.63}$$

$$Z_{j,\gamma} = \langle\psi_\gamma|c_j|\psi_\sigma\rangle \qquad R_{j,\gamma} = \langle\psi_\sigma|c_j|\psi_\gamma\rangle \tag{2.64}$$

$$\lambda_\gamma = \Delta E_\gamma \qquad \lambda_{\gamma+n_s} = -\Delta E_\gamma \tag{2.65}$$

$$S = \mathrm{diag}(+1 \quad +1 \quad \ldots \quad \mp 1 \quad \mp 1 \quad \ldots) \tag{2.66}$$

$$T = \mathrm{diag}(\underbrace{+1 \quad +1 \quad \ldots}_{n_s \text{ elements}} \quad \underbrace{\pm 1 \quad \pm 1 \quad \ldots}_{n_s \text{ elements}}) \tag{2.67}$$

for the bosonic $(-)$ and fermionic $(+)$ case and $\gamma \neq \sigma$. We omitted the zero-energy excitations $\langle\psi_\sigma|c_j|\psi_\sigma\rangle$, as they vanish in our calculations. However in general, they have to be taken into account separately from the Green's functions as in [18].

Also for the extended Q-matrix in the anomalous case, a handy relation can be calculated.

$$\begin{aligned} QSQ^\dagger &= \begin{pmatrix} R & Z \\ Z^* & R^* \end{pmatrix} \cdot \begin{pmatrix} \mathbb{I} & 0 \\ 0 & -\mathbb{I} \end{pmatrix} \cdot \begin{pmatrix} R^\dagger & Z^T \\ Z^\dagger & R^T \end{pmatrix} \\ &= \begin{pmatrix} RR^\dagger \mp ZZ^\dagger & RZ^T \mp ZR^T \\ Z^*R^\dagger \mp R^*Z^\dagger & Z^*Z^T \mp R^*R^T \end{pmatrix} \\ &= \begin{pmatrix} RR^\dagger \mp ZZ^\dagger & RZ^T \mp ZR^T \\ \mp(RZ^T \mp ZR^T)^* & \mp(RR^\dagger \mp ZZ^\dagger)^* \end{pmatrix} \\ &= S, \end{aligned} \tag{2.68}$$

where we have used the following relations for the last line

$$\begin{aligned}\left(RR^\dagger \mp ZZ^\dagger\right)_{i,j} &= \sum_\gamma \left(R_{i,\gamma}R^\dagger_{\gamma,j} \mp Z_{i,\gamma}Z^\dagger_{\gamma,j}\right) \\ &= \langle\psi_0|c_i\left(\sum_\gamma |\psi_\gamma\rangle\langle\psi_\gamma|\right)c_j^\dagger|\psi_0\rangle \mp \langle\psi_0|c_j^\dagger\left(\sum_\gamma |\psi_\gamma\rangle\langle\psi_\gamma|\right)c_i|\psi_0\rangle \\ &= \langle\psi_0^N|c_ic_j^\dagger \mp c_j^\dagger c_i|\psi_0^N\rangle \overset{(2.4)}{=} \delta_{i,j},\end{aligned} \tag{2.69}$$

$$\begin{aligned}\left(RZ^T \mp ZR^T\right)_{i,j} &= \sum_\gamma \left(R_{i,\gamma}Z_{j,\gamma} \mp Z_{i,\gamma}R_{j,\gamma}\right) \\ &= \langle\psi_0|c_i\left(\sum_\gamma |\psi_\gamma\rangle\langle\psi_\gamma|\right)c_j|\psi_0\rangle \mp \langle\psi_0|c_j\left(\sum_\gamma |\psi_\gamma\rangle\langle\psi_\gamma|\right)c_i|\psi_0\rangle \\ &= \langle\psi_0^N|c_ic_j \mp c_jc_i|\psi_0^N\rangle \overset{(2.5)}{=} 0.\end{aligned} \tag{2.70}$$

3 Basic Models

Small and relatively easy to solve systems are treated within this chapter to highlight and examine difficulties arising in various calculations. These simple calculations are comparable to exercises in quantum-mechanics courses and can therefore be found in text-books, however some procedures of solution like the treatment of anomalous (coupled) single sites with CPT might be unpublished. For the statistical-physics in chapter 3.1, we follow mainly [22].

3.1 Chemical Potential for Bosonic Systems

The chemical potential in quantum mechanics determines which states are occupied. That can be seen from the definition of grand canonical ensemble expectation values [5, p. 254]

$$\langle A\rangle = \frac{\operatorname{tr} A \exp\left(-\beta(\mathcal{H}-\mu N)\right)}{\operatorname{tr}\exp\left(-\beta(\mathcal{H}-\mu N)\right)}. \tag{3.1}$$

For zero temperature ($\beta \equiv 1/k_B T \to \infty$) this reduces to

$$\langle A\rangle = \langle\psi_0|A|\psi_0\rangle \quad \text{as } T\to 0. \tag{3.2}$$

The ground state $|\psi_0\rangle$ can be defined as the one minimizing $\langle\psi_\alpha|\mathcal{H}-\mu N|\psi_\alpha\rangle$.

If the system's Hamiltonian $\mathcal{H}$ commutes with the particle number operator N, the $|\psi_\alpha\rangle$ are eigenstates of both. Finding the ground state is therefore equivalent to minimizing $E_\alpha - \mu N_\alpha$, with the respective eigenvalues E_α and N_α.

Non-interacting Hamiltonians do not mediate between different particles, hence they contain only single-particle operators and their eigenvectors are combinations of single-particle wave-functions. Therefore the total energy E_α of an eigenstate $|\psi_\alpha\rangle$ is the sum over all energies ϵ_r of occupied single-particle states. The mean occupation of the r-th single-particle state in equilibrium is known from statistical-physics to be [22, pp. 177–178]

$$\langle n_r\rangle = \frac{1}{\exp\left(\beta(\epsilon_r-\mu)\right)\mp 1} \tag{3.3}$$

and is named Bose-Einstein ($-$) for bosonic and Fermi-Dirac distribution ($+$) for fermionic particles. For fermions, one can choose any chemical potential μ because the denominator in Eq. (3.3) stays ≥ 1 and therefore $0 \leq \langle n_r\rangle \leq 1$. The chemical potential for non-interacting, bosonic systems however, has to be chosen smaller than the smallest single-particle energy ϵ_0. Otherwise, occupation numbers would diverge

($\mu = \epsilon_0$) or even become negative ($\mu > \epsilon_0$). Although the first case leading to Bose-Einstein-condensation can be dealt with by canonical ensembles, we do not bother about it and set $\mu < \epsilon_0$ in all calculations. This means however, that such systems are empty in the zero temperature limit.

For quite generic interacting systems—for example the Bose-Hubbard model—E_α goes at least like N_α^2 as $N_\alpha \to \infty$ and one is free to choose any chemical potential.

3.2 Causality

As pointed out in chapter 2.1.4, the retarded (advanced) Green's function has to be analytical within the upper (lower) half plane. This behaviour stems from the retarded Green's function's causality. However, in nearly all calculations shown in chapter 4, we encountered—for some parameters—Green's functions, where this property was broken. To understand the underlying mechanisms, we began to investigate simple examples with similar properties. This section summarises our calculations and findings with two problems, treated by different methods.

3.2.1 Anomalous Single Bosonic Site

This is probably the simplest model with broken U(1) symmetry. It consists of a single site with an energy ϵ per particle and an additional term coupling two-particle creation- and annihilation-processes with a strength Δ. The Hamiltonian for this model is given in terms of bosonic destruction- (b) resp. creation-operators ($b^\dagger$) as

$$\mathcal{H} \equiv \epsilon b^\dagger b + \Delta \left(b^\dagger b^\dagger + bb \right), \tag{3.4}$$

which obviously does not commute with the particle number operator $N = b^\dagger b$ because

$$\left[b_i^\dagger, b_j^\dagger b_j \right] = -\delta_{i,j} b_i^\dagger, \qquad \left[b_i, b_j^\dagger b_j \right] = \delta_{i,j} b_i \tag{3.5}$$

and therefore

$$\left[b^\dagger b^\dagger + bb, b^\dagger b \right] = 2 \left(bb - b^\dagger b^\dagger \right). \tag{3.6}$$

A method often used for solving such problems is the Bogoliubov transformation [8, p. 316], where one transforms to new operators a and $a^\dagger$

$$a = ub + vb^\dagger, \qquad a^\dagger = ub^\dagger + vb, \tag{3.7}$$

with coefficients $u, v \in \mathbb{R}$ obeying $u^2 - v^2 = 1$. One can solve the system however differently, to get a better understanding of its features.

Transformation to Harmonic Oscillator

When solving the harmonic oscillator according to the ladder operator method due to Paul Dirac, one transforms the position q and momentum p operators, which obey the

commutator rule $[q, p] = \mathrm{i}$, to

$$b^\dagger = \frac{1}{\sqrt{2}}(q - \mathrm{i}p), \qquad\qquad b = \frac{1}{\sqrt{2}}(q + \mathrm{i}p). \tag{3.8}$$

We use this transformation here backwards, and substitute Eq. (3.8) into Eq. (3.4)

$$\begin{aligned}\mathcal{H} &= \frac{\epsilon}{2}(q + \mathrm{i}p)(q - \mathrm{i}p) + \frac{\Delta}{2}\left((q - \mathrm{i}p)^2 + (q + \mathrm{i}p)^2\right) \\ &= \frac{\epsilon}{2}\left(q^2 + p^2 - \mathrm{i}(qp - pq)\right) + \frac{\Delta}{2}\left(q^2 - p^2\right) \\ &= \frac{\epsilon - 2\Delta}{2}p^2 + \frac{\epsilon + 2\Delta}{2}q^2 + \frac{\epsilon}{2}.\end{aligned} \tag{3.9}$$

If we introduce $k = \epsilon + 2\Delta$ and $1/m = \epsilon - 2\Delta$, we arrive at the standard harmonic oscillator equation

$$\mathcal{H}' = \mathcal{H} - \frac{\epsilon}{2} = \frac{p^2}{2m} + \frac{kq^2}{2}, \tag{3.10}$$

whose n-th eigenstate energy is given by $E'_n = \sqrt{k/m} \cdot (n + 1/2)$. The total system has thus the eigenvalues

$$E_n = \sqrt{(\epsilon + 2\Delta)(\epsilon - 2\Delta)}\left(n + \frac{1}{2}\right) + \frac{\epsilon}{2}, \qquad n = 0, 1, 2, ... \tag{3.11}$$

We recognise that only if

$$\chi \equiv \left|\frac{\epsilon}{2\Delta}\right| \geq 1, \tag{3.12}$$

both coefficients k and m have the same sign. Otherwise, either the kinetic $p^2/2m$ or the potential energy part $kq^2/2$ is not bound from below and no physically valid ground state exists. If k and m are positive (negative), the system is a harmonic oscillator for particles (holes) and the ground state is valid. So we can identify $\chi \geq 1$ as the necessary condition for this model to be stable.

Heisenberg Equation of Motion

While the previous method showed us the physical reason for the stability condition, we will derive the time evolution of the annihilation- and creation-operators in this part and thus be able to write down the Green's function using just basic quantum mechanics.

We shall start by writing down the Heisenberg equation of motion [20, p. 50] for not explicitly time dependent operators O and $\mathcal{H}$

$$\frac{\mathrm{d}}{\mathrm{d}t}O(t) \equiv \mathrm{i}\left[\mathcal{H}, O(t)\right] = \mathrm{i}U^\dagger(t)\left[\mathcal{H}, O\right]U(t), \tag{3.13}$$

where we have pulled out the time evolution operator $U(t) = \exp(-\mathrm{i}\mathcal{H}t)$ and its Hermitian conjugate from the commutator. As we want to determine the time evolution

of annihilation- and creation-operators, it is necessary to calculate their commutators with the Hamiltonian

$$\begin{aligned}\mathcal{H}b &\overset{(3.4)}{=} \left(\epsilon b^\dagger b + \Delta(b^\dagger b^\dagger + bb)\right) b \\ &\overset{(2.4)}{=} \epsilon b(b^\dagger b - 1) + \Delta(bb^\dagger b^\dagger - 2b^\dagger + bbb) \\ &= b\left(\epsilon b^\dagger b + \Delta(b^\dagger b^\dagger + bb)\right) - \epsilon b - 2\Delta b^\dagger \\ &\overset{(3.4)}{=} b\mathcal{H} - \epsilon b - 2\Delta b^\dagger\end{aligned} \tag{3.14}$$

and analogously

$$\left[\mathcal{H}, b^\dagger\right] = \epsilon b^\dagger + 2\Delta b. \tag{3.15}$$

Plugging these results into Eq. (3.13), we derive the equations of motion for the anomalous single site problem in the form of coupled linear first order differential equations

$$\dot{b}(t) = -\mathrm{i}\epsilon b(t) - \mathrm{i}2\Delta b^\dagger(t) \tag{3.16}$$

$$\dot{b}^\dagger(t) = \mathrm{i}\epsilon b^\dagger(t) + \mathrm{i}2\Delta b(t), \tag{3.17}$$

with the initial conditions $b(0) = b$ and $b^\dagger(0) = b^\dagger$. The general solution

$$b(t) = c_1 e^{\mathrm{i}\Omega t} + c_2 e^{-\mathrm{i}\Omega t} \tag{3.18}$$

$$b^\dagger(t) = \frac{\mathrm{i}}{2\Delta}\dot{b}(t) - \frac{\epsilon}{2\Delta} b(t), \tag{3.19}$$

for this problem can be found using an exponential ansatz for $b(t)$, or by plugging Eq. (3.17) into the time-derivative of Eq. (3.16). We have introduced a generalized frequency

$$\Omega \equiv \sqrt{\epsilon^2 - (2\Delta)^2} \overset{(3.12)}{=} 2|\Delta|\sqrt{\chi^2 - 1}, \tag{3.20}$$

which is obviously closely related to the factor χ determining the models stability. If we consider the initial conditions, we end up with the solution for the time evolution of the annihilation- and creation-operator

$$b(t) = b\left(\frac{\Omega - \epsilon}{2\Omega} e^{\mathrm{i}\Omega t} + \frac{\Omega + \epsilon}{2\Omega} e^{-\mathrm{i}\Omega t}\right) - b^\dagger \mathrm{i}\frac{2\Delta}{\Omega}\sin\Omega t \equiv b\varphi_1(t) + b^\dagger\varphi_2(t) \tag{3.21}$$

$$b^\dagger(t) = b^\dagger\left(\frac{\Omega - \epsilon}{2\Omega} e^{-\mathrm{i}\Omega t} + \frac{\Omega + \epsilon}{2\Omega} e^{\mathrm{i}\Omega t}\right) + b\mathrm{i}\frac{2\Delta}{\Omega}\sin\Omega t \equiv b\psi_1(t) + b^\dagger\psi_2(t), \tag{3.22}$$

which is readily checked by insertion into the differential equations. For $\chi \geq 1$, we recognise that Ω stays real and annihilation- and creation-operator remain each other's Hermitian conjugate for all times t. For $\chi < 1$ however, $b(t)$ and $b^\dagger(t)$ diverge exponentially for $t \to \pm\infty$, indicating an unstable solution.

The retarded Green's functions have been defined via the expectation value of the commutator, which we can readily calculate having the time evolution at hand for the

normal

$$\begin{aligned} \mathrm{i}G^R(t,t') &\overset{(2.2)}{\equiv} \theta(t-t')\langle\left[b(t), b^\dagger(t')\right]\rangle \\ &\overset{(2.4)}{=} \theta(t-t')\left(\varphi_1(t)\psi_2(t') - \varphi_2(t)\psi_1(t')\right) \\ &= \theta(t-t')\left(\cos\left(\Omega(t-t')\right) - \mathrm{i}\frac{\epsilon}{\Omega}\sin\left(\Omega(t-t')\right)\right) \end{aligned} \tag{3.23}$$

and the anomalous part

$$\begin{aligned} \mathrm{i}\mathcal{F}^R(t,t') &\overset{(2.57)}{\equiv} \theta(t-t')\langle[b(t), b(t')]\rangle \\ &\overset{(2.4)}{=} \theta(t-t')\left(\varphi_1(t)\varphi_2(t') - \varphi_2(t)\varphi_1(t')\right) \\ &= \mathrm{i}\theta(t-t')\frac{2\Delta}{\Omega}\sin\left(\Omega(t-t')\right). \end{aligned} \tag{3.24}$$

For the frequency space representation, we expand sine and cosine to exponentials and use Eq. (2.12) to obtain

$$\begin{aligned} G^R(\omega) &= \frac{1}{2}\left(\frac{1}{\omega+\Omega+\mathrm{i}0^+} + \frac{1}{\omega-\Omega+\mathrm{i}0^+}\right) - \frac{\epsilon}{2\Omega}\left(\frac{1}{\omega+\Omega+\mathrm{i}0^+} - \frac{1}{\omega-\Omega+\mathrm{i}0^+}\right) \\ &= \frac{1}{2}\left(\frac{1-\epsilon/\Omega}{\omega+\Omega+\mathrm{i}0^+} + \frac{1+\epsilon/\Omega}{\omega-\Omega+\mathrm{i}0^+}\right) \\ &= \frac{(\omega+\mathrm{i}0^+)+\epsilon}{(\omega+\mathrm{i}0^+)^2-\Omega^2} \end{aligned} \tag{3.25}$$

and likewise

$$\begin{aligned} \mathcal{F}^R(\omega) &= \frac{\Delta}{\Omega}\left(\frac{1}{\omega+\Omega+\mathrm{i}0^+} - \frac{1}{\omega-\Omega+\mathrm{i}0^+}\right) \\ &= \frac{-2\Delta}{(\omega+\mathrm{i}0^+)^2-\Omega^2}. \end{aligned} \tag{3.26}$$

The poles of these Green's functions are located at $\omega_P = -\mathrm{i}0^+ \pm \Omega$ and are purely imaginary for $\chi \equiv |\epsilon/2\Delta| < 1$. Poles with positive imaginary part violate the analytical properties of retarded Green's functions derived in Chapter 2.1.4 and thus break causality. One can check numerical results for causality using Eqs. (2.31) and (2.33), which do not hold (except by chance) if the retarded Green's function contains poles in the upper half plane. An even simpler test for Green's function is possible where the Q-matrix is available, by evaluating Eq. (2.68).

Exact Solution Using CPT in Nambu Space

This way to solve the anomalous single site system could be seen as CPT of a system containing only one cluster with only one site and an anomalous perturbation V

affecting also only this single site. This treatment allows us to illustrate by a simple model, why CPT can lead to non-causal solutions.

We can rewrite Eq. (3.4) to $\mathcal{H} = \mathcal{H}_0 + V$ with

$$\mathcal{H}_0 = \epsilon b^\dagger b, \qquad V = \Delta\left(b^\dagger b^\dagger + bb\right). \tag{3.27}$$

Because $\mathcal{H}_0$ is already diagonal, we can immediately write down the time-evolutions of the annihilation- and creation-operators without perturbation

$$b(t) = be^{-\mathrm{i}\epsilon t}, \qquad b^\dagger(t) = b^\dagger e^{\mathrm{i}\epsilon t}. \tag{3.28}$$

It is also straight-forward to calculate the normal retarded Green's function with respect to $\mathcal{H}_0$ in the time- and frequency-domain, resulting in

$$G_0^R(t,t') = -\mathrm{i}\theta(t-t')e^{-\mathrm{i}\epsilon(t-t')}, \qquad G_0^R(\omega) = \left(\omega - \epsilon + \mathrm{i}0^+\right)^{-1}. \tag{3.29}$$

By introducing Nambu super-operators $\mathbf{B} \equiv \begin{pmatrix} b & b^\dagger \end{pmatrix}^{\mathrm{T}}$, the Hamiltonian can be rewritten to give

$$\begin{aligned} \mathcal{H} &= \frac{\epsilon}{2}\left(B_1^\dagger B_1 + B_2^\dagger B_2 - 1\right) + \Delta\left(B_1^\dagger B_2 + B_2^\dagger B_1\right) \\ &= \frac{1}{2}\left(\epsilon\left(\mathbf{B}^\dagger\mathbf{B} - 1\right) + \mathbf{B}^\dagger\begin{pmatrix} 0 & 2\Delta \\ 2\Delta & 0 \end{pmatrix}\mathbf{B}\right). \end{aligned} \tag{3.30}$$

The factor 1/2 was pulled out because the product of two super-operators contains $b^{(\dagger)}b^{(\dagger)}$ twice, when neglecting the order. It should also be noted, that these super-operators obey different commutator relationships $\left[B_i, B_j^\dagger\right] = \pm\delta_{i,j}$ with a positive sign for $i,j = 1$ and a negative sign for $i,j = 2$. The retarded Green's function in the super-operators contains now 4 elements—although the anomalous parts are still zero because $\mathcal{H}_0$ contains only normal components—and reads in frequency space

$$\mathcal{G}_0(\omega) = \begin{pmatrix} \omega - \epsilon + \mathrm{i}0^+ & 0 \\ 0 & -\omega - \epsilon - \mathrm{i}0^+ \end{pmatrix}^{-1}. \tag{3.31}$$

Identifying the perturbation $\mathcal{V} = \begin{pmatrix} 0 & 2\Delta \\ 2\Delta & 0 \end{pmatrix}$ within Eq. (3.30) and applying Dyson's equation Eq. (2.43) allows one to obtain the retarded Green's function for $\mathcal{H}$

$$\mathcal{G}^R(\omega) = \left(\mathcal{G}_0^{-1}(\omega) - \mathcal{V}\right)^{-1} \tag{3.32}$$

$$= \frac{1}{\left(\omega + \mathrm{i}0^+\right)^2 - \Omega^2}\begin{pmatrix} \omega + \mathrm{i}0^+ + \epsilon & -2\Delta \\ -2\Delta & -\omega - \mathrm{i}0^+ + \epsilon \end{pmatrix}, \tag{3.33}$$

where we used $\Omega = \sqrt{\epsilon^2 - (2\Delta)^2}$ again. This is the same result as Eqs. (3.25) and (3.26) because CPT is exact if $\mathcal{H}_0$ is only bilinear.

We were thus successful in obtaining an anomalous system's Green's function using CPT in Nambu space. As discussed before, means for checking the causality of Green's functions numerically are available using Eqs. (2.31) and (2.33) and applicable for this example.

3.2.2 Two Sites with Anomalous Hopping

The problem examined in this section is a little bit more sophisticated than the anomalous single site problem. It consists of two anomalously coupled sites, described by the annihilation- and creation-operators of the first $c_1^{(\dagger)}$ and second site $c_2^{(\dagger)}$. The number of particles located at site i is given by the expectation value of the particle number operator $n_i = c_i^\dagger c_i$. Instead of normal coupling, where particles can hop between the two sites resulting in $n_1 + 1$ and $n_2 - 1$ or vice versa, processes leading to $n_1 + 1$ and $n_2 + 1$ particles are considered. Problems showing a similar behaviour are for example obtained after performing a particle-hole transformation on one part of the system, while not transforming the rest. Fermionic examples are carrier generation- (recombination-) processes in semiconductors, creating (annihilating) a quasi-electron in the conduction- and a hole in the valence-band.

The bosonic Hamiltonian for this two site model is given by

$$\mathcal{H} \equiv \epsilon_1 n_1 + \epsilon_2 n_2 + \Delta \left(c_1^\dagger c_2^\dagger + c_2 c_1 \right). \tag{3.34}$$

Perturbative Solution in Nambu Space

Like before we split up the Hamiltonian into an easy to solve part $\mathcal{H}_0 = \epsilon_1 n_1 + \epsilon_2 n_2$ and the anomalous perturbation $V = \Delta \left(c_1^\dagger c_2^\dagger + c_2 c_1 \right)$ and define Nambu super-operators $\mathbf{C} \equiv \begin{pmatrix} c_1 & c_2 & c_1^\dagger & c_2^\dagger \end{pmatrix}^{\mathrm{T}}$, which allow us to write

$$\mathcal{H}_0 = \frac{1}{2} \mathbf{C}^\dagger \begin{pmatrix} \epsilon_1 & 0 & 0 & 0 \\ 0 & \epsilon_2 & 0 & 0 \\ 0 & 0 & \epsilon_1 & 0 \\ 0 & 0 & 0 & \epsilon_2 \end{pmatrix} \mathbf{C} - \frac{\epsilon_1 + \epsilon_2}{2}, \tag{3.35}$$

$$V = \frac{1}{2} \mathbf{C}^\dagger \begin{pmatrix} 0 & 0 & 0 & \Delta \\ 0 & 0 & \Delta & 0 \\ 0 & \Delta & 0 & 0 \\ \Delta & 0 & 0 & 0 \end{pmatrix} \mathbf{C} = \frac{1}{2} \mathbf{C}^\dagger \mathcal{V} \mathbf{C}, \tag{3.36}$$

where we defined the Nambu matrix $\mathcal{V}$ needed for CPT.

The solution and Green's function for the two unconnected oscillators in $\mathcal{H}_0$ are already known from Eq. (3.31) to be in Nambu space

$$\mathcal{G}_0^R(\omega) = \begin{pmatrix} \omega - \epsilon_1 + \mathrm{i}0^+ & 0 & 0 & 0 \\ 0 & \omega - \epsilon_2 + \mathrm{i}0^+ & 0 & 0 \\ 0 & 0 & -\omega - \epsilon_1 - \mathrm{i}0^+ & 0 \\ 0 & 0 & 0 & -\omega - \epsilon_2 - \mathrm{i}0^+ \end{pmatrix}^{-1}. \tag{3.37}$$

Applying Dyson's equation Eq. (2.43) yields for the total Green's function of the

system

$$G^R(\omega) = \begin{pmatrix} (z+\epsilon_2)/D_1 & 0 \\ 0 & (z+\epsilon_1)/D_2 \end{pmatrix} \tag{3.38}$$

$$\mathcal{F}^R(\omega) = \begin{pmatrix} 0 & -\Delta/D_1 \\ -\Delta/D_2 & 0 \end{pmatrix}, \tag{3.39}$$

with $z = \omega + \mathrm{i}0^+$,

$$D = z^2 + \zeta z(\epsilon_2 - \epsilon_1) - \epsilon_1\epsilon_2 + \Delta^2 \tag{3.40}$$

and $\zeta = +1$ for D_1 and -1 for D_2. The poles of the retarded Nambu Green's function $\mathcal{G} = \left(\begin{smallmatrix} G & \mathcal{F} \\ \mathcal{F}^\dagger & \bar{G} \end{smallmatrix}\right)$ are located at the roots of $D_{1,2}$

$$\omega_P = -\mathrm{i}0^+ - \zeta\frac{\epsilon_2 - \epsilon_1}{2} \pm \sqrt{\left(\frac{\epsilon_2 + \epsilon_1}{2}\right)^2 - \Delta^2}, \tag{3.41}$$

which are located in the lower half plane for

$$\chi \equiv \left|\frac{\epsilon_2 + \epsilon_1}{2\Delta}\right| \geq 1. \tag{3.42}$$

This is also the necessary condition for causality of the Green's function and stability of the model.

This calculation has been cross-checked with a numerical calculation. One can set up the infinite sized matrix of the total Hamiltonian $\mathcal{H}$ by hand, solve its eigenvalue problem numerically using a finite particle-number cut-off and compute the Q-matrix according to Eq. (2.63). The Green's functions generated by this procedure are equal to the analytical calculations for big enough cut-offs.

4 Incoherent Pumping Models

Chapter 4.1 follows quantum-optical text-books like [13, 14, 4, 31, 32, 1], while chapter 4.2 is based on [21], but the derivation of the rotating frame can also be found in many other basic text-books. The remaining chapters 4.4–4.6 contain novel work and results.

4.1 Incoherent Pumping

Pumping is the process of transmitting energy from a source to a medium. Here we will focus on a small system as medium—for example an atom or a quantum dot—interacting with a Laser wave as source. The Laser field is taken to be a monochromatic, single mode with frequency ω_L close to the excitation-energy ω_s of a state $|s\rangle$. However, generalizations to continuous spectra are possible and indeed straightforward [13, p. 478].

One must provide a way for the system under irradiance to get rid of energy. For a typical *dipole-allowed* excitation, this would come from interactions of the system with empty field modes, id est photons [4, pp. 353–354]. These interactions would allow the system to relax spontaneously and hence deplete its energy. Because of the spontaneous relaxations, the ground-state is heavily occupied and so-called population-inversion is impossible in the steady-state. Systems showing *dipole-forbidden* transitions might relax via intermediate levels or collisions. The terms dipole-allowed and -forbidden will be explained in chapter 4.1.1.

Of main interest in this thesis is the problem depicted in Fig. 4.1 (b), where an incident Laser excites dipole-forbidden transitions to the level $|s\rangle$ and the system can relax via the intermediate quantum-state $|e\rangle$, possessing a smaller excitation-energy ω_e. The dipole-allowed relaxation to the intermediate state causes the emission of a photon with energy $\omega_1 = \omega_s - \omega_e$. Upon further relaxation to the ground-state, another photon of energy $\omega_2 = \omega_e$ gets emitted. Due to the first spontaneous relaxation, the second photon will contain no information about the Laser beam's phase, motivating the term incoherent pumping.

4.1.1 Matter–Light Interactions

The following derivation of the interaction Hamiltonian is based on [13, pp. 477–485], [32, pp. 197–199] and [31, pp. 199–200].

Matter interacting with radiation may be written by the minimal coupling Hamiltonian

$$\mathcal{H} = \frac{1}{2m}\left(\boldsymbol{p} - q\boldsymbol{A}\right)^2 + V(\boldsymbol{x}) + \mathcal{H}_{rad}, \tag{4.1}$$

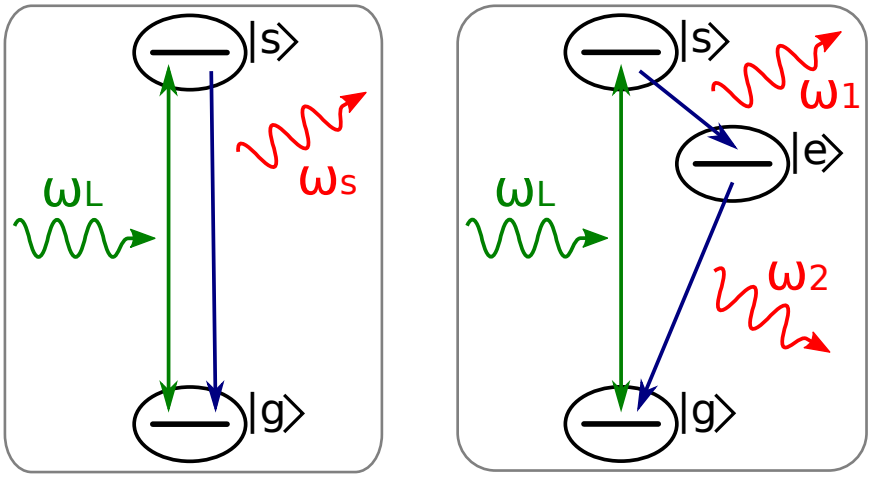

(a) Dipole transition (b) Incoherent pumping

Figure 4.1: Sketch of two different Laser excitation processes. (a) shows a Laser wave interacting with a two-level-system, possessing a dipole-allowed transition. By emitting a photon of energy $\omega_s = \omega_L$ (apart from detuning), the system can relax spontaneously. (b) depicts a Laser exciting a dipole-forbidden transition to the level $|s\rangle$. Relaxation would hence be almost impossible without the intermediate state $|e\rangle$.

within the non-relativistic limit, where q denotes the charge of a particle with a momentum operator $\boldsymbol{p}$. $V(\boldsymbol{x})$ is the potential energy, $\boldsymbol{A}$ the electro-magnetic vector-potential and $\mathcal{H}_{rad}$ the Hamiltonian describing the free radiation field.

The isolated atom without electric field can be expressed in terms of creation- and annihilation-operators $b_n^{(\dagger)}$, creating or annihilating a particle in the corresponding wave-function $\phi_n(\boldsymbol{x})$. For quantum dots, these would be the bound exciton states.

If the field is not too intense, we can neglect terms proportional to $\boldsymbol{A}^2$ in Eq. (4.1) and write the interaction Hamiltonian

$$\mathcal{H}_I \approx -\frac{q}{2m}\left(\boldsymbol{pA} + \boldsymbol{Ap}\right) = \sum_{k,n,m} g_{k,n,m}(c_k + c_k^\dagger) b_n^\dagger b_m, \tag{4.2}$$

with the coupling constant

$$g_{k,n,m} \propto \int \mathrm{d}^3\boldsymbol{x}\, \phi_n^*(\boldsymbol{x})\Big(\boldsymbol{u}_k(\boldsymbol{x})\boldsymbol{p}\Big)\phi_m(\boldsymbol{x}). \tag{4.3}$$

The creation- and annihilation-operators $c_k^{(\dagger)}$ for the radiation field, as well as the field mode function $\boldsymbol{u}_k(\boldsymbol{x})$ were introduced. The coupling constant $g_{k,n,m}$ expresses the strength, with which a photon with wave-vector k is absorbed (emitted), causing the system to jump from eigenstate ϕ_m to ϕ_n.

An important simplification of Eq. (4.2) is the so-called rotating wave approximation [4, pp. 357–358]. It neglects non-resonant terms in the expression $(c_k + c_k^\dagger) b_n^\dagger b_m$.

If the energy of the state ϕ_m is smaller than the energy corresponding to ϕ_n, $b_n^\dagger b_m$ is in fact an excitation process. The dominant (resonant) process if the system increases its energy by going from $\phi_m \to \phi_n$ is, that the electromagnetic field looses energy, hence a photon is absorbed (c_k). The term $c_k^\dagger b_n^\dagger b_m$ is nonresonant in this case and neglected within the rotating wave approximation.

Furthermore, one usually expands in Eq. (4.3) the field mode function $\boldsymbol{u}_k(\boldsymbol{x})$, which contains terms like $\exp(\mathrm{i}\boldsymbol{k}\boldsymbol{x})$. This is worthwhile because $\boldsymbol{u}_k(\boldsymbol{x})$ varies on a scale of the optical wavelength $\approx 10^{-6}\,\mathrm{m}$, while quantum systems' wave functions $\phi_n(\boldsymbol{x})$ usually vary on much smaller spatial scales—for example the Bohr radius of $\approx 10^{-11}\,\mathrm{m}$ for atoms.

In lowest order, the so-called dipole-approximation, one would stop the expansion after the first term of

$$\exp(\mathrm{i}\boldsymbol{k}\boldsymbol{x}) = 1 + \mathrm{i}\boldsymbol{k}\boldsymbol{x} + \cdots, \tag{4.4}$$

meaning $\boldsymbol{u}_k(\boldsymbol{x}) \approx \boldsymbol{u}_k(\boldsymbol{0}) = \text{const}$. By applying further the relation

$$\left[\frac{\boldsymbol{p}^2}{2m} + V(\boldsymbol{x}), \boldsymbol{x}\right] = -\mathrm{i}\frac{\boldsymbol{p}}{m}, \tag{4.5}$$

one can express the coupling constant via the dipole moment $\boldsymbol{d}_{n,m}$

$$q\int \mathrm{d}^3\boldsymbol{x}\, \phi_n^*(\boldsymbol{x})\boldsymbol{p}\phi_m(\boldsymbol{x}) = \mathrm{i}m(E_n - E_m)\underbrace{\int \mathrm{d}^3\boldsymbol{x}\, \phi_n^*(\boldsymbol{x})q\boldsymbol{x}\phi_m(\boldsymbol{x})}_{=\boldsymbol{d}_{n,m}}. \tag{4.6}$$

For dipole-allowed transitions, the dipole moment is finite and the leading contributions of the light–matter interaction can be treated within the dipole-approximation.

Dipole-forbidden transitions however, imply a vanishing dipole moment and the second order term $\mathrm{i}\boldsymbol{k}\boldsymbol{x}$ of the expansion has to be taken into account. Analogous calculations yield the electric quadrupole and the magnetic dipole moment as important factors for the coupling constant [13, pp. 172–177]. The corresponding amplitudes for these transitions are much weaker than in the dipole-allowed case. Hence spontaneous relaxations are rare and quantum-levels lacking a dipole-allowed transition are metastable. With intense Laser light however, it is possible to excite such dipole-forbidden transitions [2].

4.1.2 Application to the Present Incoherent Pumping Problem

We denote the levels again with bra- and ket-vectors $|g\rangle$, $|e\rangle$ and $|s\rangle$. Furthermore we use $c_1^{(\dagger)}$ for the creation- and annihilation-operator of photons corresponding to transitions $|s\rangle \leftrightarrow |e\rangle$, and $c_2^{(\dagger)}$ for transitions $|e\rangle \leftrightarrow |g\rangle$.

These photons will be simulated by empty, infinite baths described by Hamiltonians $\mathcal{H}_{p1}$ and $\mathcal{H}_{p2}$. As the decay processes correspond to energy dissipation, the baths must be infinite to allow the system to still decay in steady-state. This is because

finite size baths may be filled before a steady-state is reached. For simplicity, we use semi-infinite tight-binding chains for the two photon baths $i \in 1, 2$ with Hamiltonians

$$\mathcal{H}_{p,i} = \sum_{j=1}^{\infty} \omega_i c_{i,j}^\dagger c_{i,j} + t \left(c_{i,j}^\dagger c_{i,j+1} + \text{H.c.} \right), \tag{4.7}$$

where H.c. denotes the Hermitian conjugate term, t the hopping strength defining the bandwidth $B = 4t$ and ω_i the on-site energies. The operator $c_{i,j}^\dagger$ creates a photon on site j in the bath i. The semi-infinite tight-binding chain's Green's function $g^{\infty/2}$ can be expressed via the infinite tight-binding chain's green's function

$$g^{\infty/2}(l, m; \omega) = g^{\infty}(l, m; \omega) - g^{\infty}(l, -m; \omega), \tag{4.8}$$

with $l, m \in \{1, 2 \dots\}$. The expression for the infinite tight-binding chain's Green's function can be found in [5, pp. 88–98] for example.

Following Eq. (4.2), the Hamiltonian describing the spontaneous decays $|s\rangle \to |e\rangle$ and $|e\rangle \to |g\rangle$ is given by

$$V_1 \, c_{1,1}^\dagger |e\rangle\langle s| + V_2 \, c_{2,1}^\dagger |g\rangle\langle e| + \text{H.c.}, \tag{4.9}$$

with decay strengths V_1 and V_2. As pointed out in chapter 4.1.1, these decay strengths depend on the corresponding dipole moments $\boldsymbol{d}_{s,e}$ and $\boldsymbol{d}_{e,g}$.

For the Laser excitation process, we will further use the result of [4, pp. 597–601], namely that it is sufficient to treat the radiating field classically if the Laser is in a coherent mode. We can therefore write the interaction Hamiltonian for this dipole-forbidden transition as [4, p. 355]

$$\mathcal{H}_L = F e^{-\mathrm{i}\omega_L t} |s\rangle\langle g| + \text{H.c.}, \tag{4.10}$$

where the amplitude F depends on the electrical quadrupole and the magnetic dipole moment of the $|s\rangle \leftrightarrow |g\rangle$ transition, as well as on the electromagnetic field describing the Laser.

We will henceforth use $c_1^\dagger = c_{1,1}^\dagger$ and $c_2^\dagger = c_{2,1}^\dagger$, to get rid of unnecessary indices. Summing up, the total Hamiltonian of the three-level-system with incoherent pumping and spontaneous decay is given by

$$\begin{aligned} \mathcal{H} = {} & \omega_s |s\rangle\langle s| + \omega_e |e\rangle\langle e| + \mathcal{H}_{p1} + \mathcal{H}_{p2} \\ & + \left(F e^{-\mathrm{i}\omega_L t} |s\rangle\langle g| + V_1 \, c_1^\dagger |e\rangle\langle s| + V_2 \, c_2^\dagger |g\rangle\langle e| + \text{H.c.} \right). \end{aligned} \tag{4.11}$$

4.2 Rotating Frame

The Hamiltonian describing the Laser excitation Eq. (4.10) is explicitly time dependent. It is possible to remove this inconvenience by transforming into a Dirac representation with respect to

$$\mathcal{H}_0 = \omega_L \left(|s\rangle\langle s| + \sum_j c_{1,j}^\dagger c_{1,j} \right), \tag{4.12}$$

which seems to rotate with the frequency of the electrical field ω_L. The remaining Hamiltonian $\mathcal{H}_1 = \mathcal{H} - \mathcal{H}_0$ in this interaction representation is given by [21, p. 218]

$$\mathcal{H}_1^I = e^{\mathrm{i}\mathcal{H}_0 t}\mathcal{H}_1 e^{-\mathrm{i}\mathcal{H}_0 t}. \tag{4.13}$$

Let us investigate the contribution of $e^{\mathrm{i}\omega_L|s\rangle\langle s|t}$ on a state $|\alpha\rangle$, where $\alpha \in \{g, e, s\}$.

$$e^{\mathrm{i}\omega_L|s\rangle\langle s|t}|\alpha\rangle = \sum_{k=0}^{\infty} \frac{(\mathrm{i}\omega_L t)^k}{k!} \left(|s\rangle\langle s|\right)^k |\alpha\rangle \tag{4.14}$$

$$= \left(1 + \sum_{k=1}^{\infty} \frac{(\mathrm{i}\omega_L t)^k}{k!} |s\rangle\langle s|\right) |\alpha\rangle \tag{4.15}$$

$$= \begin{cases} e^{\mathrm{i}\omega_L t}|s\rangle & \text{if } \alpha = s \\ |\alpha\rangle & \text{else} \end{cases} \tag{4.16}$$

and likewise the Hermitian conjugate

$$\langle\alpha|e^{-\mathrm{i}\omega_L|s\rangle\langle s|t} = \begin{cases} e^{-\mathrm{i}\omega_L t}\langle s| & \text{if } \alpha = s \\ \langle\alpha| & \text{else.} \end{cases} \tag{4.17}$$

Because of the commutator relationships Eqs. (2.4) and (2.5), only $c_{1,j}^\dagger$ and $c_{1,j}$ transform in the Dirac representation

$$\left(c_{1,j}^\dagger\right)^I = e^{\mathrm{i}\mathcal{H}_0 t} c_{1,j}^\dagger e^{-\mathrm{i}\mathcal{H}_0 t} = c_{1,j}^\dagger e^{\mathrm{i}\omega_L t} \qquad (c_{1,j})^I = c_{1,j} e^{-\mathrm{i}\omega_L t}. \tag{4.18}$$

Putting all this together, we end up with

$$\begin{aligned} \mathcal{H}_1^I = (\omega_s - \omega_L)|s\rangle\langle s| + \omega_e|e\rangle\langle e| + \mathcal{H}_{p1}^I - \omega_L \sum_j c_{1,j}^\dagger c_{1,j} + \mathcal{H}_{p2} \\ + \left(F|s\rangle\langle g| + V_1 c_1^\dagger |e\rangle\langle s| + V_2 c_2^\dagger |g\rangle\langle e| + \text{H.c.}\right). \end{aligned} \tag{4.19}$$

From these results it is obvious, that the energy ω_s of state $|s\rangle$ as well as the photon energy ω_1 are shifted down by an amount of ω_L, as shown in Fig. 4.2.

We will henceforth use the rotating frame in most formulas and figures, as it removes the explicit time dependence and only changes two energies $\omega_s \to \omega_s - \omega_L$ and $\omega_1 \to \omega_1 - \omega_L$.

4.3 Bath Coupling

Within cluster perturbation calculations, a problem arises when modelling the spontaneous relaxation processes. As stated in Eq. (2.42), the coupling between two clusters

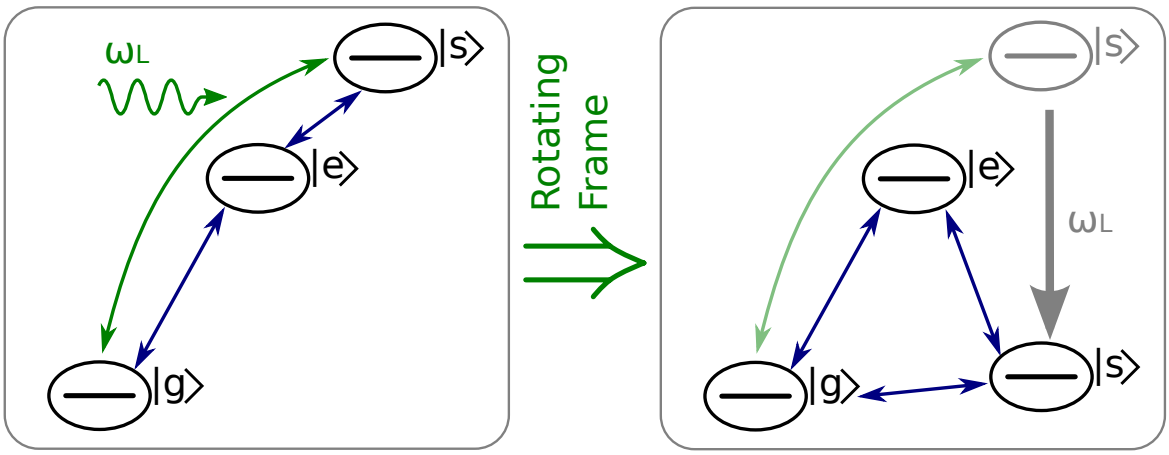

Figure 4.2: Shift of the energy level ω_s in the rotating frame.

has to be quadratic in creation- and annihilation-operators respectively. When treating the three-level-system and the photon-baths as individual clusters, the coupling for the process $|s\rangle \leftrightarrow |e\rangle$ looks like

$$V_1 c_1^\dagger |e\rangle\langle s| + \text{H.c.} \tag{4.20}$$

We could model the transitions from the ground-level $|g\rangle$ to the excited states $|e\rangle$ and $|s\rangle$ as the application of excitons' creation operators, say $b_e^\dagger$ and $b_s^\dagger$. This way, the three levels could be written as

$$|g\rangle \to |0\rangle \qquad |e\rangle \to b_e^\dagger|0\rangle \qquad |s\rangle \to b_s^\dagger|0\rangle, \tag{4.21}$$

with $|0\rangle$ defining the vacuum state, meaning no excitations present. Equation (4.20) would read

$$V_1 c_1^\dagger b_e^\dagger b_s + \text{H.c.} \tag{4.22}$$

in this representation and thus be non-quadratic. This means, CPT and VCA cannot be applied like this. We found however two possibilities to circumvent this shortcoming and apply CPT nevertheless.

The first method is probably the most obvious and simple one. We treat the photon-baths as semi-infinite tight-binding chains and combine the first sites together with the three-level-system into one cluster. The hopping towards the remaining chains is treated perturbatively and is quadratic by construction. As this method increases the state-space for diagonalising the cluster containing the three-level-system, it was not our first choice, still it is described in chapter 4.5.

Another way out of the dilemma is possible by cleverly mapping the transitions to excitons. As the influence of the Laser beam shall be taken into account exactly, processes $|g\rangle \leftrightarrow |s\rangle$ are unproblematic. However the other transitions, namely $|e\rangle \leftrightarrow |s\rangle$ and $|e\rangle \leftrightarrow |g\rangle$ must correspond to a single creation- or annihilation-operator, as we want to treat them perturbatively. This restriction can be fulfilled by identifying $|e\rangle$ as vacuum state $|0\rangle$, while $|s\rangle$ and $|g\rangle$ are treated as excitons' creation operators $b_s^\dagger$ and $b_g^\dagger$ applied on $|0\rangle$. Chapter 4.4 deals with this path.

4.4 (Not so) Cleverly Mapped Three-Level-System

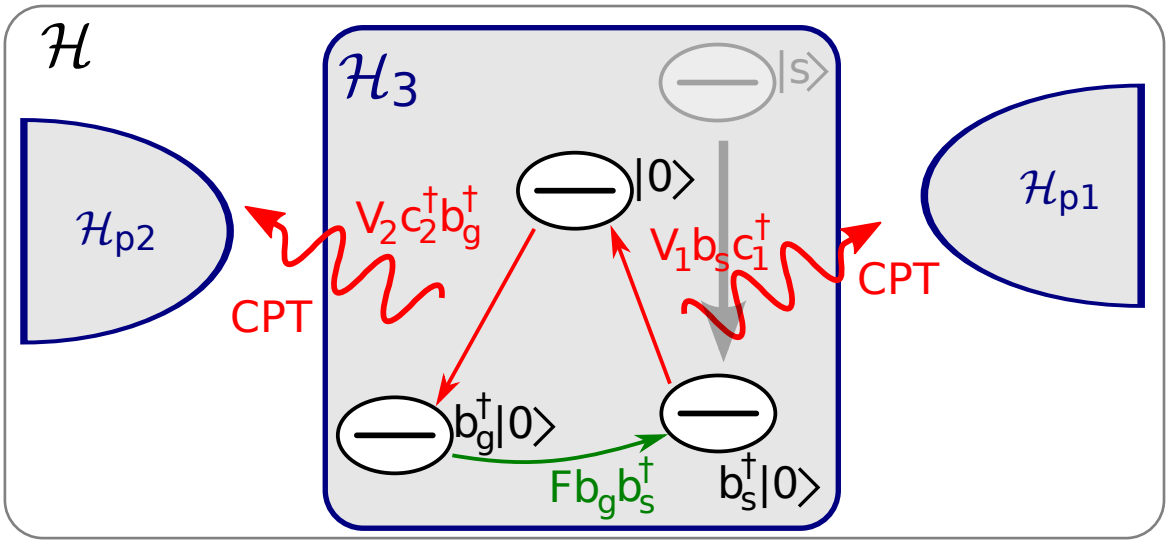

Figure 4.3: Scheme of cleverly mapped three-level-system. The red transitions are not included in $\mathcal{H}_3$, but get treated perturbatively.

Figure 4.3 shows, how the transitions are mapped to excitons, which should be treated as hard-core bosons for obeying the correct commutator relationships. Hard-core bosons are particles, which behave like bosons under permutation, but cannot occupy the same quantum state simultaneously. For convenience, we take the excitons to be interacting bosons with an interaction strength U and take the limit $U \to \infty$ at the end of our calculation. This way, they obey the usual commutator relationships and expectation values are easier to evaluate.

An alternative approach would be to map the hard-core bosons to spin-1/2 particles and perform a Jordan-Wigner transformation to spinless fermions afterwards, as for example Sachdev explains in [25, pp. 137–138,296]. However, the Jordan-Wigner fermions are non-local and could therefore complicate the couplings between three-level-system and baths.

The total system's Hamiltonian $\mathcal{H}$ in the rotating frame consists of the $U \to \infty$ limit of the three-level-system's Hamiltonian for interacting bosons

$$\mathcal{H}_{3U} = \frac{U}{2} N(N-1) + \omega_g b_g^\dagger b_g + \omega_s b_s^\dagger b_s + \left(F\, b_s^\dagger b_g + \text{H.c.}\right), \tag{4.23}$$

with the particle-number operator $N = b_g^\dagger b_g + b_s^\dagger b_s$, the bath Hamiltonians $\mathcal{H}_{p1}$ and $\mathcal{H}_{p2}$ and the quadratic coupling terms

$$V_1\, b_s^\dagger c_1 + V_2\, b_g^\dagger c_2^\dagger + \text{H.c.} \tag{4.24}$$

Mind the anomalous coupling term $b_g^\dagger c_2^\dagger$ originating from the level–exciton mapping for the ground state. Although the three cluster-Hamiltonians $\mathcal{H}_{p1}$, $\mathcal{H}_{p2}$ and $\mathcal{H}_{3U}$

commute with all particle-number operators $c_1^\dagger c_1$, $b_g^\dagger b_g$ etc., the total Hamiltonian $\mathcal{H}$ does not. By putting the only anomalous term $b_g^\dagger c_2^\dagger + \text{H.c.}$ into the CPT-coupling, it is sufficient to calculate the normal particle Green's functions G for the clusters and use them to determine the hole Green's functions $\bar{G}$ via Eqs. (2.58)–(2.59). Because the cluster-Hamiltonians contain only normal terms, their anomalous Green's functions $\mathcal{F}^{(\dagger)}$ vanish.

4.4.1 Green's Function

We define our set of basis states as

$$|n_g\, n_s\rangle = \frac{1}{\sqrt{n_g!\, n_s!}} \left(b_g^\dagger\right)^{n_g} \left(b_s^\dagger\right)^{n_s} |0\rangle, \tag{4.25}$$

with $n_g, n_s \in \{0, 1, 2\}$. It is permissible to omit states with $N > 2$, as we will take the limit $U \to \infty$ after the calculation and hence such states will not contribute to the Green's function. The $N = 2$ states however, must still be considered for calculating the Q-matrix as long as U stays finite.

As $\mathcal{H}_{3U}$ defined in Eq. (4.23) commutes with the number operator N, we can diagonalise it for every N-particle subspace separately. We label the eigenstates $|\psi_\alpha\rangle$ with corresponding eigenenergies E_α.

- $N = 0$: The only state is the vacuum with zero energy, hence

$$|\psi_1\rangle = |0\rangle \qquad\qquad E_1 = 0. \tag{4.26}$$

- $N = 1$: In this subspace, the states $|1\,0\rangle = b_g^\dagger|0\rangle$ and $|0\,1\rangle = b_s^\dagger|0\rangle$ are present. The Hamiltonian evaluates to

$$\mathcal{H}_{3U}^{(N=1)} = \begin{pmatrix} \omega_g & F^* \\ F & \omega_s \end{pmatrix}, \tag{4.27}$$

  with the eigenvalues

$$E_{2,3} = \frac{\omega_g + \omega_s}{2} \mp \sqrt{\left(\frac{\omega_g - \omega_s}{2}\right)^2 + |F|^2}. \tag{4.28}$$

  The resulting eigenvectors can be written as

$$|\psi_2\rangle = \cos\varphi |1\,0\rangle + e^{\mathrm{i}\theta} \sin\varphi |0\,1\rangle, \tag{4.29}$$

$$|\psi_3\rangle = \sin\varphi |1\,0\rangle - e^{\mathrm{i}\theta} \cos\varphi |0\,1\rangle, \tag{4.30}$$

  with $\theta = \arg(F)$ and

$$\tan\varphi = \frac{E_2 - \omega_g}{|F|}. \tag{4.31}$$

- $N = 2$: States with two particles are $|2\,0\rangle$, $|1\,1\rangle$ and $|0\,2\rangle$. As we are interested in the limit $U \to \infty$, the Hamiltonian is approximately diagonal

$$\mathcal{H}_{3U}^{(N=2)} \approx \mathrm{diag}\begin{pmatrix} U & U & U \end{pmatrix} \tag{4.32}$$

and we can set

$$|\psi_4\rangle = |2\,0\rangle \qquad |\psi_5\rangle = |1\,1\rangle \qquad |\psi_6\rangle = |0\,2\rangle, \tag{4.33}$$

each with the eigenenergy U.

By construction, the ground state ω_g must have a smaller energy than the level $|e\rangle = |0\rangle$, hence $\omega_g < 0$. Because of the rotating frame, which reduces the $|s\rangle$-level's energy by the Laser frequency ω_L, we can also identify $\omega_s < 0$.

The Q-matrix according to Eq. (2.20) for the Green's function can be calculated analytically as well. As $\omega_g, \omega_s < 0$, we first identify $|\psi_2\rangle$ with $N = 1$ as the system's ground state $|\psi_0\rangle$. Applying $b_g^\dagger$ and $b_s^\dagger$ to the ground state

$$\begin{aligned} b_g^\dagger|\psi_0\rangle &\overset{(4.29)}{=} b_g^\dagger\left(\cos\varphi|1\,0\rangle + e^{\mathrm{i}\theta}\sin\varphi|0\,1\rangle\right) \\ &= \sqrt{2}\cos\varphi|2\,0\rangle + e^{\mathrm{i}\theta}\sin\varphi|1\,1\rangle \end{aligned} \tag{4.34}$$

$$\begin{aligned} b_s^\dagger|\psi_0\rangle &\overset{(4.29)}{=} b_s^\dagger\left(\cos\varphi|1\,0\rangle + e^{\mathrm{i}\theta}\sin\varphi|0\,1\rangle\right) \\ &= \cos\varphi|1\,1\rangle + \sqrt{2}e^{\mathrm{i}\theta}\sin\varphi|0\,2\rangle, \end{aligned} \tag{4.35}$$

allows for determining the possible particle excitations

$$Q_{4,1}^\dagger \equiv \langle\psi_4|b_g^\dagger|\psi_0\rangle = \sqrt{2}\cos\varphi, \qquad Q_{5,2}^\dagger \equiv \langle\psi_5|b_s^\dagger|\psi_0\rangle = \cos\varphi, \tag{4.36}$$

$$Q_{5,1}^\dagger \equiv \langle\psi_5|b_g^\dagger|\psi_0\rangle = e^{\mathrm{i}\theta}\sin\varphi, \qquad Q_{6,2}^\dagger \equiv \langle\psi_6|b_s^\dagger|\psi_0\rangle = \sqrt{2}e^{\mathrm{i}\theta}\sin\varphi. \tag{4.37}$$

All particle-excitations contain $N = 2$ states, having energies of approximately U. For $U \to \infty$, we can neglect the energy of the ground state in the energy difference for Eq. (2.21) and write

$$\lambda_4 = \lambda_5 = \lambda_6 = U. \tag{4.38}$$

The only hole-excitations can be found by calculating

$$\begin{aligned} \langle\psi_0|b_g^\dagger &\overset{(4.29)}{=} \left(\cos\varphi\langle1\,0| + e^{-\mathrm{i}\theta}\sin\varphi\langle0\,1|\right) b_g^\dagger \\ &= \cos\varphi\langle0\,0|, \end{aligned} \tag{4.39}$$

$$\begin{aligned} \langle\psi_0|b_s^\dagger &\overset{(4.29)}{=} \left(\cos\varphi\langle1\,0| + e^{-\mathrm{i}\theta}\sin\varphi\langle0\,1|\right) b_s^\dagger \\ &= e^{-\mathrm{i}\theta}\sin\varphi\langle0\,0|, \end{aligned} \tag{4.40}$$

to be

$$Q_{7,1}^\dagger \equiv \langle\psi_0|b_g^\dagger|\psi_1\rangle = \cos\varphi, \qquad Q_{7,2}^\dagger \equiv \langle\psi_0|b_s^\dagger|\psi_1\rangle = e^{-\mathrm{i}\theta}\sin\varphi. \tag{4.41}$$

As $|\psi_1\rangle$ is the vacuum with zero energy, the energy difference is just the ground-state energy $\lambda_7 = E_2$ from Eq. (4.28).

Dropping all empty blocks of the Q-matrix, we can write it as

$$Q = \begin{pmatrix} \sqrt{2}\cos\varphi & e^{-\mathrm{i}\theta}\sin\varphi & 0 & \cos\varphi \\ 0 & \cos\varphi & \sqrt{2}e^{-\mathrm{i}\theta}\sin\varphi & e^{\mathrm{i}\theta}\sin\varphi \end{pmatrix}, \tag{4.42}$$

with $S = \operatorname{diag}\begin{pmatrix} 1 & 1 & 1 & -1 \end{pmatrix}$ and $\lambda = \begin{pmatrix} U & U & U & E_2 \end{pmatrix}^T$. From Eq. (2.24), we know that $QSQ^\dagger$ should evaluate to the identity. This can be used to check our calculations.

$$\begin{aligned} Q \cdot S \cdot Q^\dagger &= Q \cdot \begin{pmatrix} 1 & & & \\ & 1 & & \\ & & 1 & \\ & & & -1 \end{pmatrix} \cdot \begin{pmatrix} \sqrt{2}\cos\varphi & 0 \\ e^{\mathrm{i}\theta}\sin\varphi & \cos\varphi \\ 0 & \sqrt{2}e^{\mathrm{i}\theta}\sin\varphi \\ \cos\varphi & e^{-\mathrm{i}\theta}\sin\varphi \end{pmatrix} \\ &= \begin{pmatrix} \sqrt{2}\cos\varphi & e^{-\mathrm{i}\theta}\sin\varphi & 0 & \cos\varphi \\ 0 & \cos\varphi & \sqrt{2}e^{-\mathrm{i}\theta}\sin\varphi & e^{\mathrm{i}\theta}\sin\varphi \end{pmatrix} \cdot \begin{pmatrix} \sqrt{2}\cos\varphi & 0 \\ e^{\mathrm{i}\theta}\sin\varphi & \cos\varphi \\ 0 & \sqrt{2}e^{\mathrm{i}\theta}\sin\varphi \\ -\cos\varphi & -e^{-\mathrm{i}\theta}\sin\varphi \end{pmatrix} \\ &= \begin{pmatrix} 2\cos^2\varphi + \sin\varphi - \cos\varphi & 0 \\ 0 & \cos^2\varphi + \cos\varphi - \sin\varphi \end{pmatrix} = \begin{pmatrix} 1 & 0 \\ 0 & 1 \end{pmatrix} \end{aligned} \tag{4.43}$$

Using Eqs. (2.18) and (2.29) we are now capable of calculating the full Keldysh-space Green's function $\hat{g}_{0\,3,3}$ for the three-level-system in equilibrium and at $T = 0$. Its retarded component for example has the elements

$$g^R_{0\,3,3} \triangleq \begin{pmatrix} (b_g, b_g^\dagger) & (b_g, b_s^\dagger) \\ (b_s, b_g^\dagger) & (b_s, b_s^\dagger) \end{pmatrix}. \tag{4.44}$$

As already pointed out before, the hole Green's function $\bar{\hat{g}}_{0\,3,3}$ is also readily evaluated from $\hat{g}_{0\,3,3}$ using Eqs. (2.58)–(2.59).

4.4.2 Coupling the Baths to the Three-Level-System

The calculation here is very similar to the example given in chapter 2.2. The main differences are, that now three clusters are coupled together and the Green's functions are defined in Nambu space.

Like the total Hamiltonian consists of the three cluster-Hamiltonians, the Green's function before CPT does as well

$$\mathcal{G}_0 = \operatorname{diag}\begin{pmatrix} \hat{g}_{0\,1,1} & \hat{g}_{0\,2,2} & \hat{g}_{0\,3,3} & \bar{\hat{g}}_{0\,1,1} & \bar{\hat{g}}_{0\,2,2} & \bar{\hat{g}}_{0\,3,3} \end{pmatrix}. \tag{4.45}$$

In this 6-by-6-cluster Nambu-space, the normal perturbation $V_1\, b_s^\dagger c_1 + \text{H.c.}$ mediates particle $\hat{g}_{0\,1,1}$ with particle Green's function $\hat{g}_{0\,3,3}$ and hole $\bar{\hat{g}}_{0\,1,1}$ with hole Green's function $\bar{\hat{g}}_{0\,3,3}$. The anomalous perturbation $V_2\, b_g^\dagger c_2^\dagger + \text{H.c.}$ however connects particle with hole terms and vice versa, explicitly $\hat{g}_{0\,2,2}$ with $\bar{\hat{g}}_{0\,3,3}$ and $\bar{\hat{g}}_{0\,2,2}$ with $\hat{g}_{0\,3,3}$.

Putting all this in matrix form, the CPT equation (2.44) looks like

$$\mathcal{G}^{-1} \overset{(2.44)}{=} \mathcal{G}_0^{-1} - V = \begin{pmatrix} \hat{g}_{0\,1,1}^{-1} & & -\hat{V}_1 & & & \\ & \hat{g}_{0\,2,2}^{-1} & & & & -\hat{V}_2 \\ -\hat{V}_1 & & \hat{g}_{0\,3,3}^{-1} & & -\hat{V}_2 & \\ & & & \bar{\hat{g}}_{0\,1,1}^{-1} & & -\hat{V}_1 \\ & & -\hat{V}_2 & & \bar{\hat{g}}_{0\,2,2}^{-1} & \\ & -\hat{V}_2 & & -\hat{V}_1 & & \bar{\hat{g}}_{0\,3,3}^{-1} \end{pmatrix}. \tag{4.46}$$

This matrix contains two non-communicating blocks, indicated by light-blue and black elements. Therefore the matrix is block-diagonal and we can just focus on one of the sub-matrices, say the black one. One can also reorder the indices to cluster-1-particle, cluster-2-hole and cluster-3-particle and invert the whole equation to finally get

$$\hat{G} = \begin{pmatrix} \hat{G}_{1,1} & \cdots & \hat{G}_{1,3} \\ \cdots & \bar{\hat{G}}_{2,2} & \hat{\mathcal{F}}_{2,3} \\ \cdots & \cdots & \hat{G}_{3,3} \end{pmatrix} = \begin{pmatrix} \hat{g}_{0\,1,1}^{-1} & & -\hat{V}_1 \\ & \bar{\hat{g}}_{0\,2,2}^{-1} & -\hat{V}_2 \\ -\hat{V}_1 & -\hat{V}_2 & \hat{g}_{0\,3,3}^{-1} \end{pmatrix}^{-1}. \tag{4.47}$$

The inverse of the right-hand 3-by-3 matrix can be readily calculated. We are especially interested in the $(3,3)$ element, which evaluates to

$$\hat{G}_{3,3} = \left((\hat{g}_{0\,3,3})^{-1} - \hat{\Sigma} \right)^{-1}, \tag{4.48}$$

with the self-energy-like Keldysh-space matrix $\hat{\Sigma}$, whose elements are defined as

$$\Sigma^{R/A/K} = g_{0\,1,1}^{R/A/K} \cdot V_1^2 \cdot \begin{pmatrix} 0 & 0 \\ 0 & 1 \end{pmatrix} + \bar{g}_{0\,2,2}^{R/A/K} \cdot V_2^2 \cdot \begin{pmatrix} 1 & 0 \\ 0 & 0 \end{pmatrix}. \tag{4.49}$$

The 2-by-2 matrices stem from the fact, that V_1 couples cluster one ($c_1^\dagger$) to the $|s\rangle$-state (b_s), which is the (2,2)-element of the three-level Green's function, while V_2 couples cluster two ($c_2^\dagger$) to the $|g\rangle$-state ($b_g^\dagger$).

4.4.3 Results

Solving for the Keldysh-component of Eq. (4.48), we are able to calculate the "particle densities" n_g and n_s with the help of Eq. (2.36). They should correspond in our picture to the probabilities of the system residing in state $|g\rangle$ and $|s\rangle$. The probability for state $|e\rangle$ can be calculated as $n_e = 1 - n_g - n_s$ because our system has only three-levels.

Calculations show however, that the sum $n_g + n_s > 1$ in a huge parameter regime, which would mean $n_e < 0$. It is obvious that we cannot interpret a negative probability and we have to admit our method's failure. For small decay strengths V_1 and V_2, n_g is shown in Fig. 4.4. The particle density n_s evaluates to approximately $0.61 n_g$ for this calculation. Therefore the density n_e is negative in the whole regime, except for $V_1 \approx 0$, where it is zero. It is interesting, that not even for such small couplings, the method is working as intended.

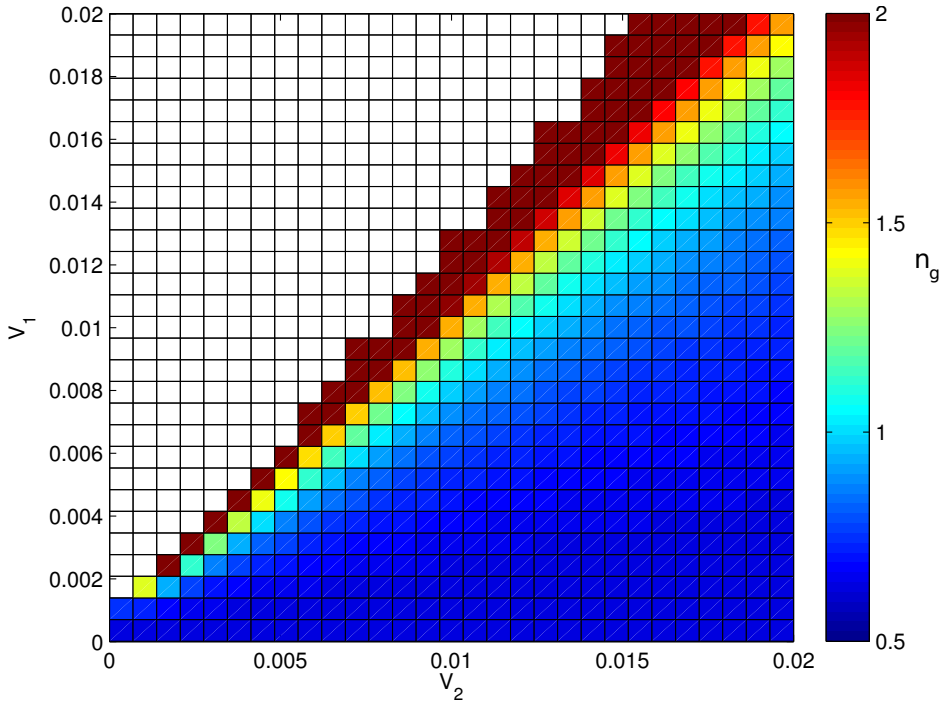

Figure 4.4: Particle density $n_g = \langle b_g^\dagger b_g \rangle$ for the cleverly mapped three-level-system as a function of the coupling constants V_1 and V_2. For white areas, the system behaves unstable. The other parameters are listed in the table.

The problem originates from the fact, that we chose the highest state $|e\rangle$ as a vacuum state. Choosing $|g\rangle$ would have been more appropriate, however we would have been unable to apply CPT in this case, as already discussed in chapter 4.3. Therefore we focused our further efforts on the alternative treatment described in chapter 4.5.

Here we present the calculation of all interesting quantities exemplary for one special set of parameters:

ω_L	ω_e	ω_s	ω_1	ω_2	F	V_1	V_2
1.9	1	2	$\omega_s - \omega_e$	ω_e	0.2	0.35	0.5

In the rotating frame, we end up with $\omega_s = 0.1$ and $\omega_1 = -0.9$. The baths are semi-infinite tight-binding chains with constant on-site energies of ω_1 and ω_2, hopping strengths $t = 1$ and chemical potentials $\mu_1 = \mu_2 = -10$. This is way below the lowest state, which would have an energy of $\omega_i - 2t$.

The sum rule Eq. (2.33) for the three-level-system's green's function $G^R_{3,3}$ after CPT is fulfilled up to an error of 10^{-4}, while the relationship

$$\int_{-\infty}^{\infty} \mathrm{d}\omega \, \left(G^R(\omega)\right)^2 \stackrel{!}{=} 0, \tag{4.50}$$

necessary for the Green's function's causality Eq. (2.31) has a similar error of 10^{-4}. While the quantities $n_g = 0.88$ and $n_s = 0.54$ are too high for $n_e > 0$, we can still calculate for example the photon densities on the first bath-sites, yielding $n_1 = n_2 = 0.07$. The quantity 0^+ for the three-level-system was taken to be 10^{-6} for these results and the interaction strength was set to $U = 100$.

4.5 Reference System Containing Bath Sites

After finding out about the problems of the not so cleverly mapped three-level-system (confer chapter 4.4.3), we followed an alternative path. It was clear from the previous calculations, that mapping an excited level to the vacuum state would only cause inconvenience and causality difficulties. Our solution for this issue was to treat the three-level-system with all excitation- and emission-processes exactly and apply CPT to the photon-dissipation systems, id est "cut" the photon-baths.

In Fig. 4.5, the three clusters are portrayed, where one site of every bath—here $c_1^\dagger$ from bath 1 and $c_2^\dagger$ from bath 2—are incorporated within the central cluster. This central cluster's Hamiltonian

$$\begin{aligned} \mathcal{H}_{3+} = \omega_s |s\rangle\langle s| + \omega_e |e\rangle\langle e| + \sum_i \omega_i c_i^\dagger c_i \\ + \left(F|s\rangle\langle g| + V_1 c_1^\dagger |e\rangle\langle s| + V_2 c_2^\dagger |g\rangle\langle e| + \text{H.c.} \right) \end{aligned} \tag{4.51}$$

does not commute any more with the particle number operators $\hat{n}_i = c_i^\dagger c_i$ for $i \in \{1, 2\}$. Therefore the Green's functions would have to be calculated in the whole Nambu space

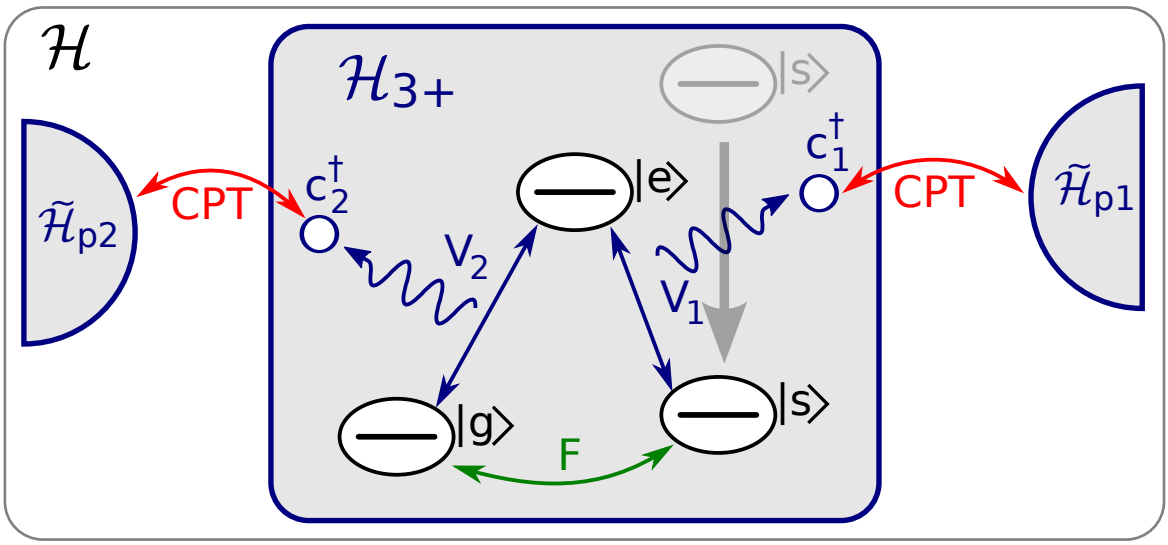

Figure 4.5: Scheme of the three-level-system with incorporated bath sites. The red transitions are treated perturbatively.

according to Eq. (2.61). But there is another conserved quantity, which we introduce in chapter 4.5.1 and can be used to reduce the effort for calculating the Green's functions.

The Hamiltonians $\tilde{\mathcal{H}}_{p,i}$ of the baths without their first sites and the couplings T_i, connecting them to the central cluster are given by

$$\tilde{\mathcal{H}}_{p,i} = \sum_{j=2}^{\infty} \omega_i c_{i,j}^\dagger c_{i,j} + t\left(c_{i,j}^\dagger c_{i,j+1} + \text{H.c.}\right), \qquad T_i = t\left(c_i^\dagger c_{i,2} + \text{H.c.}\right). \tag{4.52}$$

4.5.1 Problematic Ground State

Because of the rotating frame, ω_s and $\omega_1 \equiv \omega_s - \omega_e$ are reduced by the Laser frequency ω_L. As ω_L is close to the excitation energy ω_s, the photon energy ω_1 comes out be negative. Similarly to chapter 3.1, the ground-state would have a diverging particle number of these photons and an infinite negative energy.

As $\mathcal{H}_{3+}$ does not commute with the particle number operators, it is not feasible to introduce a chemical potential to circumvent this problem. This would complicate the calculation enormously because $\mathcal{H}_{3+}$ and N share no common set of eigenstates. However, one can find another operator of a conserved quantity

$$\tilde{N} = |e\rangle\langle e| + \hat{n}_2 - \hat{n}_1. \tag{4.53}$$

Proof. The only non-trivial parts of the commutator $\left[\tilde{N}, \mathcal{H}_{3+}\right]$ are

$$\begin{aligned}
&(|e\rangle\langle e| + \hat{n}_2)\left(c_2^\dagger|g\rangle\langle e| + c_2|e\rangle\langle g|\right) \\
&\qquad = c_2|e\rangle\langle g| + \underbrace{\hat{n}_2 c_2^\dagger}_{c^\dagger\hat{n}+c^\dagger}|g\rangle\langle e| + \underbrace{\hat{n}_2 c_2}_{c\hat{n}-c}|e\rangle\langle g| \\
&\qquad = \left(c_2^\dagger\hat{n}_2 + c_2^\dagger\right)|g\rangle\langle e| + c_2\hat{n}_2|e\rangle\langle g| \\
&\qquad = \left(c_2^\dagger|g\rangle\langle e| + c_2|e\rangle\langle g|\right)(|e\rangle\langle e| + \hat{n}_2)
\end{aligned} \tag{4.54}$$

and

$$\begin{aligned}
&(|e\rangle\langle e| - \hat{n}_1)\left(c_1^\dagger|e\rangle\langle s| + c_1|s\rangle\langle e|\right) \\
&\qquad = c_1^\dagger|e\rangle\langle s| - \underbrace{\hat{n}_1 c_1^\dagger}_{c^\dagger\hat{n}+c^\dagger}|e\rangle\langle s| \underbrace{-\hat{n}_1 c_1}_{c-c\hat{n}}|s\rangle\langle e| \\
&\qquad = -c_1^\dagger\hat{n}_1|e\rangle\langle s| + (c_1\hat{n}_1 + c_1)|s\rangle\langle e| \\
&\qquad = \left(c_1^\dagger|e\rangle\langle s| + c_1|s\rangle\langle e|\right)(|e\rangle\langle e| - \hat{n}_1)\,.
\end{aligned} \tag{4.55}$$

This means $\left[\tilde{N}, \mathcal{H}_{3+}\right] = 0$ and therefore $\langle\tilde{N}\rangle$ is a conserved quantity. □

It is possible to introduce a chemical-potential-like quantity $\tilde{\mu}$ now and use it together with the operator $\tilde{N}$ for selecting a different "ground-state" by minimizing the expectation value of the generalized free energy $F = \mathcal{H}_{3+} - \tilde{\mu}\tilde{N}$. In fact, this corresponds to reordering the eigenstates from sorted in energy to sorted in $\langle F\rangle$. This procedure is valid because we are doing non-equilibrium calculations and are free to let our system evolve from any arbitrary state. This means, our three-level-system is *not* in an equilibrium situation before CPT-coupling. Hence we cannot apply the equilibrium relations derived from Eq. (2.25) to calculate the Keldysh from the retarded Green's function.

The differences between the Hamiltonian $\mathcal{H}_{3+}$ and the free energy F are

$$\omega_e\,|e\rangle\langle e| \quad \rightarrow \quad (\omega_e - \tilde{\mu})\,|e\rangle\langle e| \tag{4.56}$$

$$\omega_2\,\hat{n}_2 \quad \rightarrow \quad (\omega_2 - \tilde{\mu})\,\hat{n}_2 \tag{4.57}$$

$$\omega_1\,\hat{n}_1 \quad \rightarrow \quad (\omega_1 + \tilde{\mu})\,\hat{n}_1. \tag{4.58}$$

Realizing that $\omega_2 - \tilde{\mu} > 0$ and $\omega_1 + \tilde{\mu} > 0$ must hold for a finite ground-state energy, we can derive the following boundaries for $\tilde{\mu}$:

$$\tilde{\mu} < \omega_2 \equiv \omega_e \tag{4.59}$$

$$\tilde{\mu} > -\omega_1 = -(\omega_s - \omega_2) = \omega_e - \omega_s = \omega_e - \delta \tag{4.60}$$

In the rotating frame, ω_s is reduced by the Laser frequency ω_L and thus similar to the detuning δ, which is the difference between the atom's excitation energy and the

Laser frequency. We are therefore left with a narrow region to choose our generalized chemical potential $\tilde{\mu}$. If $\delta < 0$, id est the Laser frequency is higher than the atom's level spacing, Eqs. (4.59) and (4.60) cannot be fulfilled simultaneously and one has to come up with a different solution. Probably interchanging $|s\rangle$- and $|g\rangle$-states would be enough.

In fact, the region for $\tilde{\mu}$ is too small for many parameters to gain a good ground-state, where a good ground-state is characterized by containing only a small number of photons n_1 and n_2. The reason for this will become evident in chapter 4.5.2. For such cases, we will just choose one eigenstate with a low amount of photons and treat it as the system's initial state.

4.5.2 Green's Function

We choose our set of basis states as

$$|\alpha\, n_2\, n_1\rangle = \frac{1}{\sqrt{n_2!\, n_1!}} \left(c_2^\dagger\right)^{n_2} \left(c_1^\dagger\right)^{n_1} |\alpha\, 0\, 0\rangle, \tag{4.61}$$

with $\alpha \in \{g, e, s\}$ and $n_i \in \{0, 1, 2 \ldots N_i^{cut}\}$. The boson numbers get cut-off at N_i^{cut} because the Hamiltonian is non-trivial to solve. The number of non-zero elements in $\mathcal{H}_{3+}$ grows like $3d$ (see below), with the basis' dimension $d = 3(N_1^{cut}+1)(N_2^{cut}+1)$.

It is easy to calculate the Hamiltonian's action on an arbitrary basis state

$$\mathcal{H}_{3+}|g\, n_2\, n_1\rangle = F|s\,..\rangle + V_2\sqrt{n_2}|.\, n_2 - 1\,.\rangle + \sum \omega_i n_i|\ldots\rangle \tag{4.62}$$

$$\mathcal{H}_{3+}|s\, n_2\, n_1\rangle = F^*|g\,..\rangle + V_1\sqrt{n_1+1}|..\, n_1+1\rangle + \left(\omega_s + \sum \omega_i n_i\right)|\ldots\rangle \tag{4.63}$$

$$\mathcal{H}_{3+}|e\, n_2\, n_1\rangle = V_1\sqrt{n_1}|..\, n_1 - 1\rangle + V_2\sqrt{n_2+1}|.\, n_2+1\,.\rangle + \left(\omega_e + \sum \omega_i n_i\right)|\ldots\rangle, \tag{4.64}$$

where a dot (.) indicates no change in the corresponding level (g, s, e) or photon count (n_1, n_2). This means, the Hamilton matrix contains at most three elements in every column and hence it growths like $3d$.

For reasonable cut-offs, the Hamiltonian contains more elements, than analytical methods can handle. The Hamiltonian is therefore solved numerically and used to calculate the Q-matrix, according to Eq. (2.63). Retarded and Keldysh Green's functions $\mathcal{G}_{0\,3+}^{R/K}$ are then computable from Eqs. (2.61)–(2.62) for the included bath-sites c_1 and c_2. We defined the retarded and Keldysh Green's functions of the central cluster as having the elements

$$\mathcal{G}_{0\,3+}^{R/K} \triangleq \begin{pmatrix} (c_1, c_1^\dagger) & (c_1, c_1) & (c_1, c_2^\dagger) & (c_1, c_2) \\ (c_1^\dagger, c_1^\dagger) & (c_1^\dagger, c_1) & (c_1^\dagger, c_2^\dagger) & (c_1^\dagger, c_2) \\ & & & \\ (c_2, c_1^\dagger) & (c_2, c_1) & (c_2, c_2^\dagger) & (c_2, c_2) \\ (c_2^\dagger, c_1^\dagger) & (c_2^\dagger, c_1) & (c_2^\dagger, c_2^\dagger) & (c_2^\dagger, c_2) \end{pmatrix}. \tag{4.65}$$

4.5.3 CPT Coupling

The CPT matrix-equation, Eq. (2.44) is very simple in this case, as long as we mind the Keldysh- and Nambu-space structures. The coupling matrices T_i contain just normal elements and couple via normal hopping the first site of bath 1 to the $(1,1)$- and the first site of bath 2 to the $(2,2)$-subspace of $\mathcal{G}_{0\,3+}$.

The calculation goes by analogy with the example in chapter 2.2 and—for completeness—yields

$$\left(\mathcal{G}^R_{3+}\right)^{-1} = \left(\mathcal{G}^R_{0\,3+}\right)^{-1} - \Sigma^R \tag{4.66}$$

$$\mathcal{G}^K_{3+} = \mathcal{G}^R_{3+}\left(\left(\mathcal{G}^{-1}_{0\,3+}\right)^K - \Sigma^K\right)\mathcal{G}^A_{3+}, \tag{4.67}$$

with

$$\Sigma^{R/K} = t^2 \begin{pmatrix} \mathcal{G}^{R/K}_{0\,1,1} & 0 \\ 0 & \mathcal{G}^{R/K}_{0\,2,2} \end{pmatrix}. \tag{4.68}$$

4.5.4 Results

Here we treat the calculation of all interesting quantities exemplary for the following set of parameters before transforming into the rotating frame:

ω_L	ω_e	ω_s	ω_1	ω_2	F	V_1	V_2	N_1^{cut}	N_2^{cut}
1.9	1	2	$\omega_s - \omega_e$	ω_e	0.2	0.35	0.5	6	6

In the rotating frame, we end up with $\omega_s = 0.1$ and $\omega_1 = -0.9$. The baths are semi-infinite tight-binding chains with constant on-site energies of ω_1 and ω_2, hopping strengths $t = 1$ and chemical potentials $\mu_1 = \mu_2 = -10$. This is way below the lowest state, which would have an energy of $\omega_i - 2t$.

We choose our initial state $|\psi_I\rangle$ to be the eigenstate with the smallest number of photons of $n_1 = 0.24$ and $n_2 = 0.22$, being

$$|\psi_I\rangle = 0.747 \cdot |g\,0\,0\rangle - 0.480 \cdot |s\,0\,0\rangle + 0 \cdot |e\,0\,0\rangle \cdots . \tag{4.69}$$

That means, with a norm of 0.89, it consists only of $n_1 = n_2 = 0$ states. As it also contains small amounts of states having a photon count close or equal to the cut-offs, Eq. (2.68) claiming $QSQ^\dagger = S$ is only fulfilled with an error of about 10^{-6}, which is good enough for our purposes.

The sum rule Eq. (2.33) for the three-level-system's Green's function G^R_{3+} after CPT is fulfilled up to an error of $5 \cdot 10^{-4}$, while the relationship

$$\int_{-\infty}^{\infty} \mathrm{d}\omega \, \left(G^R(\omega)\right)^2 \stackrel{!}{=} 0, \tag{4.70}$$

stemming from the Green's function's causality Eq. (2.31) has an error of $4 \cdot 10^{-2}$. This deviation is quite big, but if we continue nevertheless with our calculation, we end up with finite photon densities after CPT of $n_1 = n_2 = 0.14$. The quantity 0^+ was chosen as being 10^{-4} for these results. The photon current into bath 2 evaluates to $I_{3,2} = 1.06$.

4.6 Single Site Approximation

Generating and solving the Hamiltonian Eq. (4.51) in section 4.5, calculating the Q-matrix, applying CPT and integrating the resulting Green's functions numerically is time consuming. There are also many parameters to tune, namely the level energies, Laser strength as well as detuning and relaxation rates. Furthermore, only some parameter regimes give causal Green's functions and it is cumbersome to find them using this approach.

A more convenient way is to solve the pure three-level-system without relaxation processes exactly and approximate it with a single bosonic site, communicating via CPT with the baths. Most of the calculation can be performed analytically, so checking a lot of parameters for causality is easily possible and very fast. While this method is not exact, it gives at least a an idea for which results to expect.

4.6.1 Green's Function and Approximation

We start by writing down the pure three-level-system's Hamiltonian in the rotating frame

$$\mathcal{H}_3 = \omega_s|s\rangle\langle s| + \omega_e|e\rangle\langle e| + (F|s\rangle\langle g| + \text{H.c.})\,, \tag{4.71}$$

which contains no spontaneous relaxations any more. The Hamilton matrix for the order $|g\rangle$, $|s\rangle$, $|e\rangle$ is

$$\mathcal{H}_3 = \begin{pmatrix} 0 & F^* & 0 \\ F & \omega_s & 0 \\ 0 & 0 & \omega_e \end{pmatrix}, \tag{4.72}$$

so only the two lowest levels $|g\rangle$ and $|s\rangle$ are connected and the eigenenergies are easily calculable to give

$$E_{0,1} = \frac{\omega_s}{2} \mp \sqrt{\left(\frac{\omega_s}{2}\right)^2 + |F|^2}, \qquad E_2 = \omega_e. \tag{4.73}$$

The resulting eigenvectors can be written as

$$|\psi_0\rangle = \cos\varphi|g\rangle + e^{\mathrm{i}\theta}\sin\varphi|s\rangle, \tag{4.74}$$
$$|\psi_1\rangle = \sin\varphi|g\rangle - e^{\mathrm{i}\theta}\cos\varphi|s\rangle, \tag{4.75}$$
$$|\psi_2\rangle = |e\rangle, \tag{4.76}$$

with $\theta = \arg(F)$ and $\tan\varphi = E_0/|F|$.

Of course, the linear set of equations (4.74), (4.75) can be inverted to give

$$|g\rangle = \cos\varphi|\psi_0\rangle + \sin\varphi|\psi_1\rangle, \tag{4.77}$$
$$|s\rangle = e^{-\mathrm{i}\theta}\left(\sin\varphi|\psi_0\rangle - \cos\varphi|\psi_1\rangle\right). \tag{4.78}$$

Plugging these relations into the perturbation from the spontaneous relaxation processes Eq. (4.9) yields

$$\mathcal{V} = V_1\, c_1^\dagger |e\rangle\langle s| + V_2\, c_2^\dagger |g\rangle\langle e| + \text{H.c.} \tag{4.79}$$

$$\begin{aligned} &= \left(e^{\mathrm{i}\theta} V_1 \sin\varphi\, c_1^\dagger |\psi_2\rangle\langle\psi_0| + \cos\varphi V_2\, c_2 |\psi_2\rangle\langle\psi_0| + \text{H.c.}\right) \\ &- \left(e^{\mathrm{i}\theta} V_1 \cos\varphi\, c_1^\dagger |\psi_2\rangle\langle\psi_1| - \sin\varphi V_2\, c_2 |\psi_2\rangle\langle\psi_1| + \text{H.c.}\right). \end{aligned} \tag{4.80}$$

For $V_1, V_2 = 0$, the ground and only occupied state would be $|\psi_0\rangle$. If V_1, V_2 would be small with respect to the detuning, $|\psi_1\rangle$ would be nearly unoccupied and we could neglect the third line in the above equation. Actually this is never the case as the detuning is usually small. However, we neglect this line nevertheless just for the sake of simplicity.

With the perturbation containing only the states $|\psi_0\rangle$ and $|\psi_2\rangle$, we can ignore the third state $|\psi_1\rangle$ and map the three-level-system on a single bosonic site $b^\dagger$ with an on-site energy $\epsilon = E_2 - E_0$. The Hamiltonian $\mathcal{H}_{3\sim} = \epsilon b^\dagger b$ is now very simple and the Green's function is known to be $g^R_{0\,3,3} = 1/(\omega - \epsilon + \mathrm{i}0^+)$.

4.6.2 CPT Coupling

The perturbation reduces in this approximation to

$$\tilde{V}_1\, c_1^\dagger b^\dagger + \tilde{V}_2\, c_2 b^\dagger + \text{H.c.}, \tag{4.81}$$

with modified coupling constants

$$\tilde{V}_1 = e^{\mathrm{i}\theta} V_1 \sin\varphi, \qquad \tilde{V}_2 = \cos\varphi V_2. \tag{4.82}$$

This yields a CPT matrix-equation equal to Eq. (4.46), with the only difference that $\hat{V}_i = \tilde{V}_i \cdot \left(\begin{smallmatrix} 1 & 0 \\ 0 & 1 \end{smallmatrix}\right)$ in Keldysh-space. Under inversion, the important elements evaluate to

$$\hat{G}_{i,i} = \left((\hat{g}_{0\,i,i})^{-1} - \hat{\Sigma}_i \right)^{-1}, \tag{4.83}$$

with $i \in \{1, 2, 3\}$ and self-energy-like Keldysh-space matrices $\hat{\Sigma}_i$ defined as

$$\hat{\Sigma}_1 = \tilde{V}_1^2 \cdot \left(\left(\hat{\tilde{g}}_{0\,3,3}\right)^{-1} - \tilde{V}_2^2 \cdot \hat{\tilde{g}}_{0\,2,2} \right)^{-1}, \tag{4.84}$$

$$\hat{\Sigma}_2 = \tilde{V}_2^2 \cdot \left((\hat{g}_{0\,3,3})^{-1} - \tilde{V}_1^2 \cdot \hat{\tilde{g}}_{0\,1,1} \right)^{-1}, \tag{4.85}$$

$$\Sigma_3^{R/A/K} = \bar{g}_{0\,1,1}^{R/A/K} \cdot \tilde{V}_1^2 + g_{0\,2,2}^{R/A/K} \cdot \tilde{V}_2^2. \tag{4.86}$$

These equations allow for calculating photon densities n_1 and n_2 in the baths as well as the occupation n_3 of the single site by evaluating Eq. (2.36).

For calculating the photon-current $I_{3,2}$, flowing from the three-level-system to bath 2, we need the Keldysh part of $\hat{G}_{3,2}$, which can be obtained from $\hat{G}_{3,3}$ and $\hat{g}_{0\,2,2}$ as

$$G^R_{3,2} = G^R_{3,3} \cdot \tilde{V}_2 \cdot g^R_{0\,2,2}, \tag{4.87}$$

$$G^K_{3,2} = G^R_{3,3} \cdot \tilde{V}_2 \cdot g^K_{0\,2,2} + G^K_{3,3} \cdot \tilde{V}_2 \cdot g^A_{0\,2,2}. \tag{4.88}$$

Integrating $G^K_{3,2}$ over ω as in Eq. (2.37) yields the $t = 0$ Green's function, whose real part is proportional to the current, as Eq. (2.41) shows.

4.6.3 Results

To check the total system's stability, it is sufficient to search for poles of $G^R_{3,3}$ in the upper half plane. If they exist, the Green's function after CPT is not causal and thus the system will not be stable. Applying Eqs. (4.83) and (4.86), this is equivalent to finding complex roots z_0 with a positive imaginary part $\operatorname{Im} z_0 > 0$ of

$$\left(G^R_{3,3}(z_0)\right)^{-1} = z_0 - \epsilon + \mathrm{i}0^+ - \bar{g}^R_{0\,1,1}(z_0) \cdot \tilde{V}_1^2 - g^R_{0\,2,2}(z_0) \cdot \tilde{V}_2^2 \stackrel{!}{=} 0. \tag{4.89}$$

In Fig. 4.6, the stability of the total system is shown for logarithmic bath Green's functions of the form

$$g(\omega) = \frac{1}{B - A} \log \frac{\omega - A}{\omega - B}. \tag{4.90}$$

The spectral function, defined in Eq. (2.35) for this type of Green's functions is rectangular within $\omega \in [A, B]$. Obviously from the figure, a necessary but not sufficient condition for a stable solution is $\tilde{V}_2 > \tilde{V}_1$.

The particle density of the single bosonic site for stable solutions is plotted in Fig. 4.7. If approximating the three-level-system with the single site would be valid, these numbers would correspond one-on-one to the occupation probability in the excited state $|e\rangle$. This is not the case, as was already pointed out in chapter 4.6.1. Therefore, the particle density $\langle b^\dagger b \rangle$ is only an approximation for the occupation probability in $|e\rangle$. Nevertheless, we can find stable regions with high activity by applying this simple approximation and calculate the correct numbers with the method described in chapter 4.5.

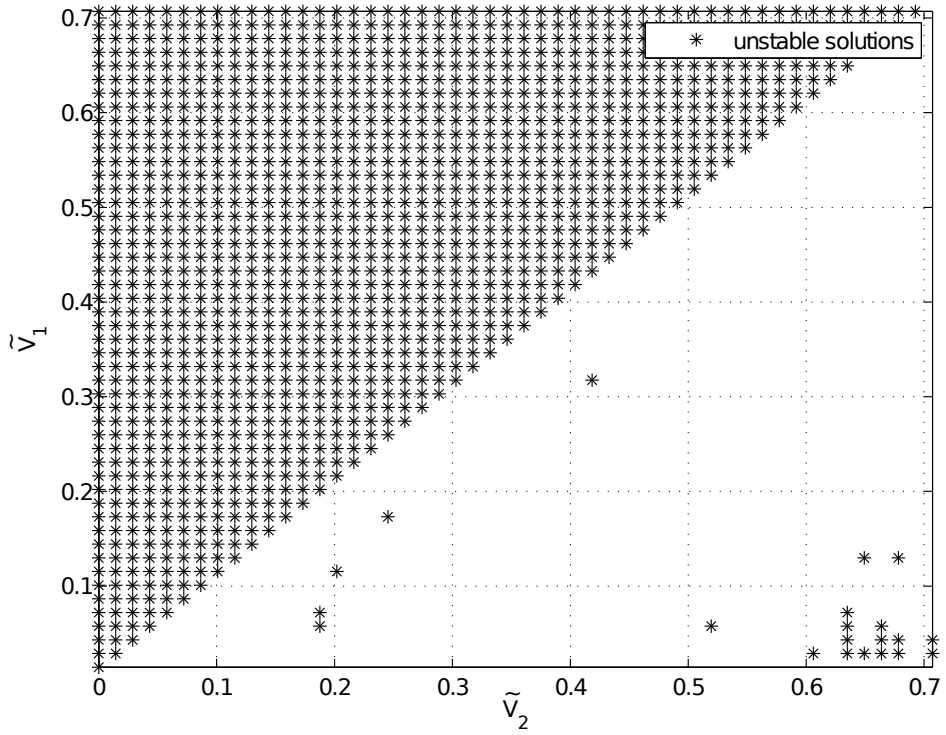

Figure 4.6: Unstable solutions for the total three-level-system within the single-site approximation are marked with an asterisk as a function of the modified coupling constants $\tilde{V}_1$ and $\tilde{V}_2$. The on-site energy ϵ was set to 1.2 and $B = -A = 1$ was used. The main feature, that no stable solutions exist for $\tilde{V}_1 > \tilde{V}_2$ remains valid for different parameters.

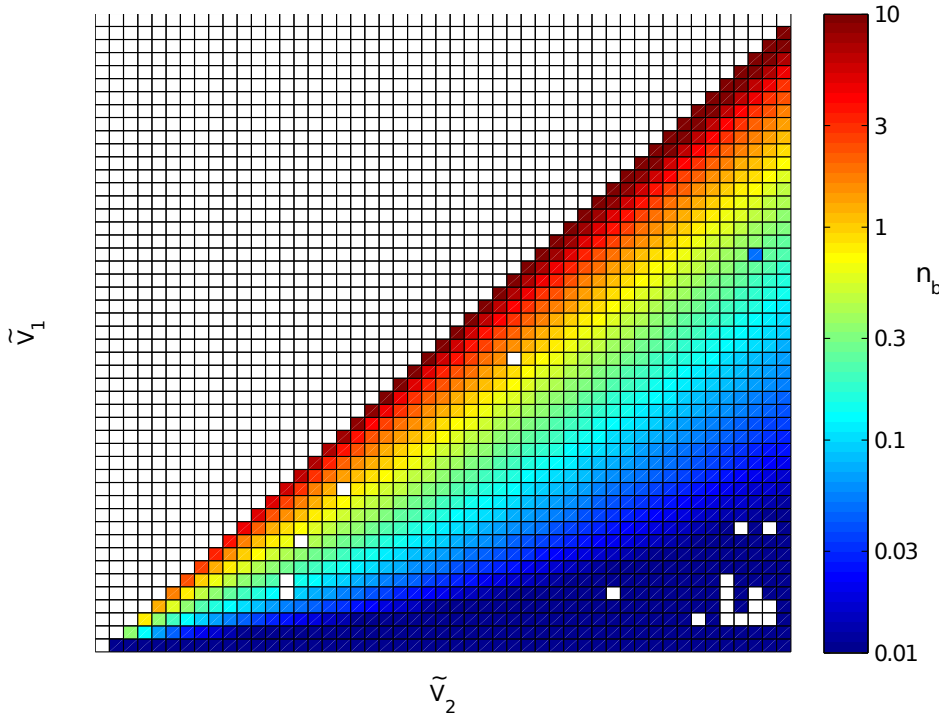

Figure 4.7: Particle density $n_b = \langle b^\dagger b \rangle$ of stable solutions for the single-site approximation as a function of the modified coupling constants $\tilde{V}_1$ and $\tilde{V}_2$. The on-site energy ϵ was set to 1.2 and $B = -A = 1$ was used.

5 Conclusion

The aim of this thesis was to describe optical pumping processes with methods from theoretical solid-state physics. Cluster perturbation theory (CPT), a predecessor of the more modern variational cluster approach (VCA), was used together with non-equilibrium Keldysh Green's functions. Possible applications for the incoherent pumping models derived in this work would be the description of many-body phenomena in Laser-driven optical microcavity-systems.

We investigated some specialities of bosonic systems in chapter 3. Namely the problem of the chemical potential with non-interacting Hamiltonians and Green's functions' causalities and their correspondence to stability. Their understanding was of vital importance for the further calculations.

In chapter 4, we derived three variants for describing incoherent optical pumping by means of CPT. The calculations are easily extensible to VCA. The currently most promising method consists of exactly diagonalising one bath-site together with the three-level-system and treating the remaining baths perturbatively.

By approximating the action of the three-level-system on the baths with a single bosonic site, we were able to obtain a simple and analytically handleable model. It enabled us to quickly scan through a vast range of parameters and look for stable solutions.

The third method presented in this thesis relies on remapping the three-level-system's levels to hard-core excitons. While encountering a lot of problems along this calculation and having to drop the originally intended meaning of the excitons, we were nevertheless able to calculate photon densities for some special cases. However, these numbers are to be treated only with caution.

Although the computation of a single, Laser-driven three-level-system was successful in the end, for the calculation of complete photonic crystals with many impurities under Laser irradiation a lot more work has to be done.

Acknowledgements

First of all, I would like to thank my supervisor Prof. Enrico Arrigoni for his effort and patience in trying to make me understand the quantum-world. All the discussions on simple models, basic ideas, problems and results were very challenging, but even the more interesting. I would also like to thank Prof. Wolfgang von der Linden for his contributions in our weekly group-meetings.

I feel greatly in the whole many-body group's depth for "stealing" so much of their time and knowledge with my endless questions. I especially owe gratitude to Michael Knap, for boosting my learning curve with his explanations. But also Martin Nuss, Anna Fulterer, Christoph Heil and Faruk Geles were a great help in discussing countless issues of quantum mechanics, computer sciences and which film to watch next.

I am exceedingly grateful for my family and their support. Finally, I would like to express my love and affection for Andrea because she listens to me, even though I am talking about quantum mechanics :)

Bibliography

[1] L. Bergmann and C. Schaefer. *Optik – Wellen- und Teilchenoptik*, volume 3 of *Lehrbuch der Experimentalphysik*. Walter de Gruyter, 10th edition, 2004.

[2] M. Bhattacharya, C. Haimberger, and N. P. Bigelow. Forbidden transitions in a magneto-optical trap. *Physical Review Letters*, 91:213004, Nov 2003.

[3] C. Clausen, I. Usmani, F. Bussieres, N. Sangouard, M. Afzelius, H. de Riedmatten, and N. Gisin. Quantum storage of photonic entanglement in a crystal. *Nature*, 469(7331):508–511, Jan. 2011.

[4] C. Cohen-Tannoudji, J. Dupont-Roc, and G. Grynberg. *Atom-photon interactions: Basic processes and applications*. Wiley-VCH, 2004.

[5] E. Economou. *Green's functions in quantum physics*. Springer Series in Solid-State Sciences. Springer, 2006.

[6] A. Faraon. Stanford University, 2012.

[7] A. Faraon, I. Fushman, D. Englund, N. Stoltz, P. Petroff, and J. Vučković. Coherent generation of non-classical light on a chip via photon-induced tunnelling and blockade. *Nature Physics*, 4(11):859–863, 2008.

[8] A. Fetter and J. Walecka. *Quantum theory of many-particle systems*. Dover Books on Physics. Dover Publications, 2003.

[9] C. Gros and R. Valentí. Cluster expansion for the self-energy: A simple many-body method for interpreting the photoemission spectra of correlated fermi systems. *Physical Review B*, 48:418–425, Jul 1993.

[10] H. Haug and A. Jauho. *Quantum kinetics in transport and optics of semiconductors*. Number 6 in Springer Series in Solid-State Sciences. Springer, 2008.

[11] K. Hennessy, A. Badolato, P. Petroff, and E. Hu. Positioning photonic crystal cavities to single InAs quantum dots. *Photonics and Nanostructures - Fundamentals and Applications*, 2(2):65–72, 2004.

[12] K. Hennessy, A. Badolato, M. Winger, D. Gerace, M. Atature, S. Gulde, S. Falt, E. L. Hu, and A. Imamoglu. Quantum nature of a strongly coupled single quantum dot-cavity system. *Nature*, 445(7130):896–899, Feb. 2007.

[13] I. Hertel and C. Schulz. *Atome, Moleküle und optische Physik 1.* Springer, 1st edition, 2008.

[14] I. Hertel and C. Schulz. *Atome, Moleküle und optische Physik 2.* Springer, 1st edition, 2010.

[15] S. John. Strong localization of photons in certain disordered dielectric superlattices. *Physical Review Letters*, 58:2486–2489, Jun 1987.

[16] L. Keldysh. Diagram technique for nonequilibrium processes. *Zhurnal Eksperimentalnoi i Teoreticheskoi Fiziki*, 47(1515), 1964.

[17] M. Knap, E. Arrigoni, and W. von der Linden. Spectral properties of strongly correlated bosons in two-dimensional optical lattices. *Physical Review B*, 81:024301, 2010.

[18] M. Knap, E. Arrigoni, and W. von der Linden. Variational cluster approach for strongly correlated lattice bosons in the superfluid phase. *Physical Review B*, 83:134507, 2011.

[19] M. Knap, W. von der Linden, and E. Arrigoni. Nonequilibrium steady state for strongly correlated many-body systems: Variational cluster approach. *Physical Review B*, 84:115145, 2011.

[20] J. Negele and H. Orland. *Quantum many-particle systems.* Advanced Books Classics. Westview Press, 1998.

[21] W. Nolting. *Quantenmechanik – Grundlagen*, volume 5/1 of *Grundkurs Theoretische Physik.* Springer, 7th edition, 2009.

[22] W. Nolting. *Statistische Physik*, volume 6 of *Grundkurs Theoretische Physik.* Springer, 6th edition, 2009.

[23] M. Potthoff, M. Aichhorn, and C. Dahnken. Variational cluster approach to correlated electron systems in low dimensions. *Physical Review Letters*, 91:206402, 2003.

[24] J. Rammer and H. Smith. Quantum field-theoretical methods in transport theory of metals. *Reviews of Modern Physics*, 58(2):323–359, 1986.

[25] S. Sachdev. *Quantum phase transitions*, volume 2. Cambridge University Press, 2011.

[26] D. Sénéchal. An introduction to quantum cluster methods. arXiv:0806.2690v2 [cond-mat.str-el], 2010.

[27] D. Sénéchal, D. Perez, and M. Pioro-Ladrière. Spectral weight of the hubbard model through cluster perturbation theory. *Physical Review Letters*, 84:522–525, 2000.

[28] D. Sénéchal, D. Perez, and D. Plouffe. Cluster perturbation theory for hubbard models. *Physical Review B*, 66:075129, Aug 2002.

[29] J. Vučković and Y. Yamamoto. Photonic crystal microcavities for cavity quantum electrodynamics with a single quantum dot. *Applied Physics Letters*, 80:2374, 2003.

[30] E. Waks and J. Vučković. Dipole induced transparency in drop-filter cavity-waveguide systems. *Physical Review Letters*, 96:153601, Apr 2006.

[31] D. Walls and G. Milburn. *Quantum Optics*. Springer, 1st edition, 1995.

[32] D. Walls and G. Milburn. *Quantum Optics*. Springer, 2nd edition, 2008.

[33] E. Yablonovitch. Inhibited spontaneous emission in solid-state physics and electronics. *Physical Review Letters*, 58:2059–2062, May 1987.

[34] T. Yoshie, A. Scherer, J. Hendrickson, G. Khitrova, H. M. Gibbs, G. Rupper, C. Ell, O. B. Shchekin, and D. G. Deppe. Vacuum rabi splitting with a single quantum dot in a photonic crystal nanocavity. *Nature*, 432(7014):200–203, Nov. 2004.

Index